phenanthridin-5(4H)-one (HA-718), and 4-butyl-11-(1,1,1,3,3, 3-hexafluoro-2-hydroxypropan-2-yl)-[1,3]dioxolo[4,5-c]phenan-thridin-5(4H)-one (HA-718), and 4-butyl-11-(1,1,1,3,3,3-hexa-fluoro-2-hydroxypropan-2-yl)-7-methoxy-[1,3]dioxolo[4,5-c] phenanthridin-5(4H)-one (HA-719) (Fig. 1) proved to be highly potent and selective inhibitors of HCV (genotype 1b) replication. KZ-16, HA-718, and HA-719 reduced luciferase activity and viral RNA copy number in LucNeo#2 cells in a dose-dependent fashion (Fig. 2A–C). However, they did not affect the viability of Huh-7.5.1 cells at concentrations up to 40 μM (Fig. 2D). When the cytotoxicity of the compounds was evaluated by the copy number of GAPDH mRNA in the host cells, a similar result was obtained (data not shown).

Table 1 summarizes the anti-HCV activity of KZ-16, HA-718, and HA-719 in different (genotype 1b) replicon cells and in Huh-7 cells infected with cell-free JFH1 (genotype 2a) virus. The highest activity was achieved by HA-719 followed by KZ-16 and HA-718. The $EC_{50}$ of KZ-16, HA-718, and HA-719 were $0.13 \pm 0.04$, $0.23 \pm 0.06$, and $0.063 \pm 0.010$ μM, respectively, in LucNeo#2 cells, when determined by the luciferase reporter activity. The 50% cytotoxic concentrations ($CC_{50}$) of all compounds were >40 μM. Therefore, the selectivity indices (SI), based on the ratio of $CC_{50}$ to $EC_{50}$, of KZ-16, HA-718, and HA-719 were >307, >173, and >634, respectively. The anti-HCV activity of these compounds was confirmed by reduction of the viral RNA copy number in different replicon cells. However, they were less potent inhibitors of genotype 2a HCV (JFH1) replication in cell-free virus infection assay. Furthermore, the phenanthridinone derivatives were much less active in Huh-7 cells transfected with JFH1 replicons than in genotype 1b replicon cells (data not shown).

Immunoblot analysis was conducted to confirm that phenanthridinone derivatives were inhibitory to the expression of NS3 and NS5A proteins of HCV. As shown in Fig. 3, HA-719 strongly inhibited NS3 and NS5A expression in LucNeo#2 cells in a dose dependent fashion without affecting the expression of the host cellular protein GAPDH. The compound achieved 93% and 86% inhibition of NS3 and

NS5A, respectively, at a concentration of 0.5 μM, indicating that HA-719 is a potent inhibitor of HCV protein expression as well as viral RNA synthesis. Immunoblot analysis was also conducted for another phenanthridinone derivative, 2-(2-benzyloxy-1,1,1,3,3,3-hexafluoropropan-2-yl)-5-butyl-3-methoxyphenanthridin-6(5H)-one (KZ-37), of which anti-HCV activity was weaker than HA-719. KZ-37 also proved inhibitory to NS3 and NS5A expression in a dose-dependent fashion (data not shown).

In our attempt to elucidate the mechanism of action of the compounds, HA-719 was examined for their ability to inhibit the enzymatic activity of genotype 1b NS3 protease and NS5B polymerase in cell-free assay systems. Little, if any, inhibition of NS3 protease activity was observed for HA-719. Its 50% inhibitory concentration ($IC_{50}$) for the protease was 5.7 μM (data not shown), which was much higher than its $EC_{50}$ for HCV replication in replicon cells (0.063–0.44 μM). HA-719 did not show any inhibitory effect on NS5B polymerase activity at concentrations up to 20 μM (data not shown). Furthermore, KZ-37, of which $EC_{50}$ for HCV replication was 2.1–4.8 μM, was inactive against these two enzymes at a concentration of 20 μM (data not shown). Thus, it is unlikely that the phenanthridinone derivatives suppress HCV replication by inhibiting the activity of either NS3 protease or NS5B polymerase.

## 4. Discussion

In this study, we have demonstrated that novel phenanthridinone derivatives are potent and selective inhibitors of HCV replication in vitro. Our previous study on the synthesis and antiviral activity of phenanthridinone derivatives demonstrated that some of them exhibited selective but moderate activity against HCV replication in replicon cells [20,21]. After optimization of chemical structures, we succeeded in obtaining a series of potent and selective derivatives (Fig. 1). Among them, the most active one was HA-719, a novel phenanthridinone derivative with a dioxole structure.

Previous studies of HCV replicon cell systems indicated that most replicons had cell culture-adaptive mutations, which arose during the selection process with G418 and enhanced replication efficiency [26–29]. Self-replicating subgenomic RNA replicons could be eliminated from Huh-7 cells by prolonged treatment with IFN, and a higher frequency of cured cells could support the replication of subgenomic and full-genomic replicons [30]. The replication efficiency decreased with increasing amounts of transfected replicon RNA, indicating that viral RNA or proteins are cytopathic or that host cell factors in Huh-7 cells limit RNA amplification [31]. Therefore, both viral and cellular factors are considered to be important determinants for the efficiency of HCV replication in cell cultures, which may be able to explain the difference in $EC_{50}$ values of the compounds among the subgenomic replicon cells used in this study (Table 1). Similarly, the difference in $EC_{50}$ values in subgenomic and full-genomic replicon cells might be due to the difference of HCV RNA length or the difference of the host cells [32]. In fact, shorter RNA is known to replicate more efficiently than longer one [33].

The activity of phenanthridinone derivatives against the genotype 2a strain JFH1 was weaker than that against genotype 1b (Table 1). Although the assay systems were not the same (replicon cell assay for genotype 1b versus cell-free virus infection assay for genotype 2b), the compounds were much less active against genotype 2a (Table 1 and data not shown). Such difference in drug-sensitivity between genotype 1b and genotype 2a was previously reported and attributed to the genetic heterogeneity within the HCV genome [23]. In addition, the anti-HCV activity of compounds had been optimized in the genotype 1b replicon cells. HCV is classified into 6 genotypes that are further separated into a series of subtypes [34,35]. Among the genotypes, genotype 1b virus is epidemiologically predominant in Japan, and 65 and 17% of the cases
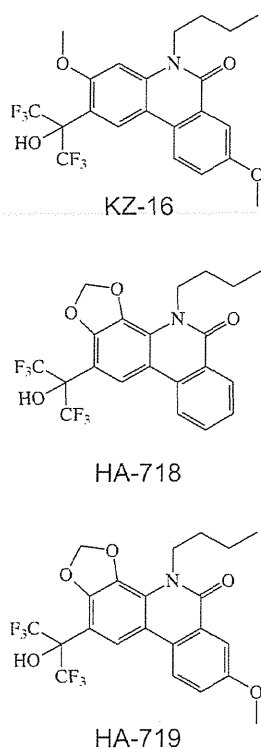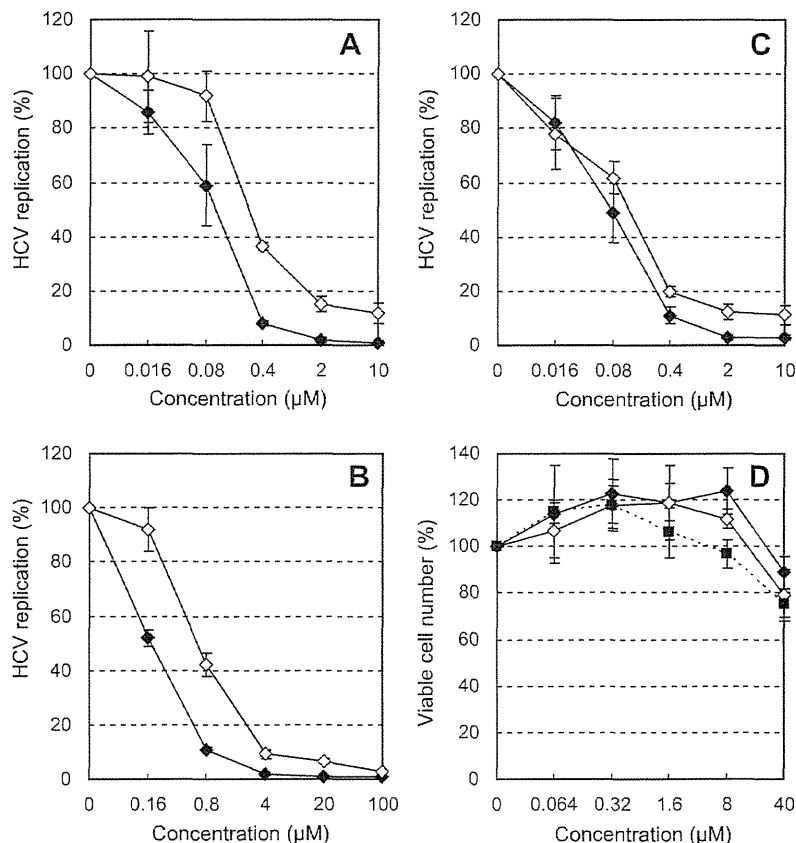


Fig. 1. Chemical structures of phenanthridinone derivatives.

Fig. 2. Inhibitory effect of phenanthridinone derivatives on the replication HCV RNA replicons in LucNeo#2 cells and the proliferation of Huh-7 cells. LucNeo#2 cells were cultured in the presence of various concentrations of (A) KZ-16, (B) HA-718, or (C) HA-719. After incubation for 3 days, the cells were subjected to luciferase assay (closed diamond) and real-time RT-PCR (open diamond) to measure replicon-associated luciferase activity and RNA copy number, respectively, as parameters of HCV replication. (D) For the cell proliferation assay, Huh-7 cells were cultured in the presence of various concentrations of KZ-16 (closed diamond), HA-718 (open diamond), or HA-719 (closed square). After incubation for 3 days, the number of viable cells was determined by a tetrazolium dye method. Data represent means ± SD for triplicates experiments. Experiments were repeated at least twice, and a representative result is shown.

Table 1
Anti-HCV activity of phenanthridinone derivatives.

| Compound | | $EC_{50}$ (μM) | | | | | $CC_{50}$ (μM) |
|---|---|---|---|---|---|---|---|
| | Virus genotype | 1b | | | | 2a | |
| | Cell | LucNeo#2 | | #50–1 | NNC#2 | Huh-7.5.1 | Huh-7 |
| | Assay | Luciferase | Real-time RT-PCR | | | | Tetrazolium |
| KZ-16 | | 0.13 ± 0.04 | 0.28 ± 0.01 | 0.40 ± 0.12 | 0.40 ± 0.14 | 2.6 ± 0.9 | >40 |
| HA-718 | | 0.23 ± 0.06 | 0.68 ± 0.02 | 0.97 ± 0.56 | 0.90 ± 0.44 | 14 ± 5 | >40 |
| HA-719 | | 0.063 ± 0.010 | 0.14 ± 0.01 | 0.25 ± 0.05 | 0.44 ± 0.20 | 4.9 ± 2.2 | >40 |
| CsA | | 0.24 ± 0.05 | 0.16 ± 0.01 | 0.18 ± 0.03 | N.D. | 0.58 ± 0.01 | 12 ± 3 |

$EC_{50}$: 50% effective concentration; $CC_{50}$: 50% cytotoxic concentration. N.D.: not determined.

Antiviral assay against the genotype 2a HCV was evaluated by the infection of Huh-7.5.1 cells with cell-free JFH-1 virus (see Section 2).

Except for the results in NNC#2 cells, all data represent means ± SD for three independent experiments. The data in NNC#2 cells represent means ± ranges for two independent experiments.

of HCV-related chronic hepatitis were caused by genotype 1b and genotype 2b, respectively [36].

At present, the target molecule of our phenanthridinone derivatives for inhibition of HCV replication remains unknown. Although it cannot be completely excluded that the compounds are inhibitors of NS3 protease or NS5B polymerase, biochemical assays revealed that HA-719 proved not to inhibit the activity of these enzymes at the concentrations capable of inhibiting viral replication. Therefore, the compounds may interact with another non-structural protein essential for viral replication, such as NS3

helicase and NS5A. In fact, a highly active inhibitor targeting NS5A has recently been identified [37]. Alternatively, the phenanthridinone derivatives may inhibit HCV replication through the interaction with host cellular factors deeply involved in HCV replication process [38–40]. It was reported that PJ34, a phenanthridinone derivative, had immunomodulatory activities and was protective against autoimmune diabetes [41], liver cancer [42], and stroke [43]. These studies suggested that the effects of PJ34 were attributed to the inhibition of poly(ADP-ribose) polymerase (PARP). Therefore, HA-719 was tested for its inhibitory effect on
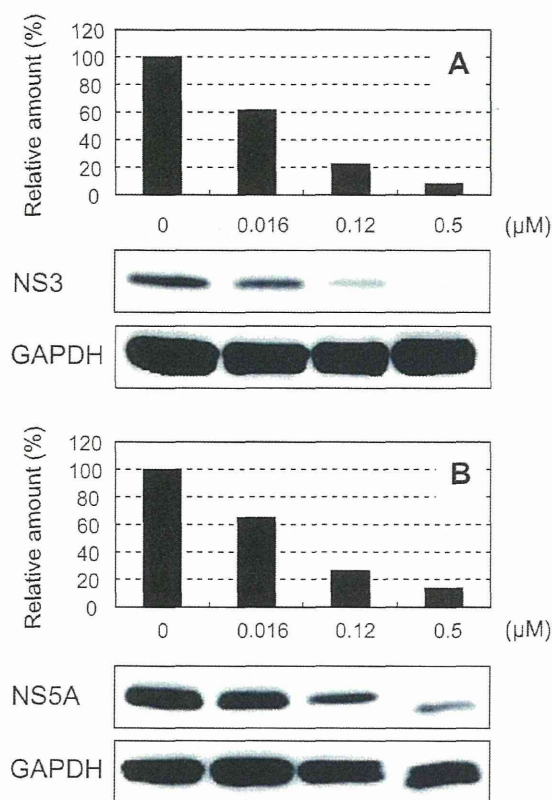
**Fig. 3.** Inhibitory effect of HA-719 on the expression of HCV proteins in LucNeo#2 cells. The cells were cultured in the presence of various concentrations of the compound. After incubation for 4 days, the cells were subjected to electrophoresis and immunoblot analysis for expression of (A) NS3 and (B) NS5A proteins. The band images were quantified by an image scanner and densitometer. Experiments were repeated at least twice, and a representative result is shown.

PARP activity and found to be inactive (data not shown). It was reported that some phenanthridinone derivatives had anti-human immunodeficiency virus (HIV) activity through the inhibition of viral integrase [44]. However, our compounds did not show selective inhibition of HIV replication in cell cultures (data not shown). Further studies, including the establishment of drug-resistant replicons, are in progress to determine the mechanism of action of the phenanthridinone derivatives.

In conclusion, our results clearly demonstrate that the novel phenanthridinone derivatives, especially HA-719, are highly potent and selective inhibitors of HCV replication in vitro. Although further studies, such as determination of their target molecule and pharmacological properties in vivo, are required, this class of compounds should be pursued for their clinical potential in the treatment of HCV infection.

### Acknowledgments

### References

[1] M. Koziel, M. Peters, Viral hepatitis in HIV infection, N. Engl. J. Med. 356 (2007) 1445–1454.

[2] J.H. Hoofnagle, Course and outcome of hepatitis C, Hepatology 36 (2002) S21–29.

[3] P. Sharma, A. Lok, Viral hepatitis and liver transplantation, Semin. Liver Dis. 26 (2006) 285–297.

[4] A.M. Di Bisceglie, J.H. Hoofnagle, Optimal therapy of hepatitis C, Hepatology 36 (2002) S121–127.

[5] M.W. Fried, M.L. Shiffman, K.R. Reddy, C. Smith, G. Marinos, F.L. Jr Gonçales, D. Häussinger, M. Diago, G. Carosi, D. Dhumeaux, A. Craxi, A. Lin, J. Hoffman, J. Yu, Peginterferon alfa-2a plus ribavirin for chronic hepatitis C virus infection, N. Engl. J. Med. 347 (2002) 975–982.

[6] A. Craxi, A. Licata, Clinical trial results of peginterferons in combination with ribavirin, Semin. Liver Dis. 23 (1) (2003) 35–46.

[7] Q.L. Choo, G. Kuo, A.J. Weiner, L.R. Overby, D.W. Bradley, M. Houghton, Isolation of a cDNA clone derived from a blood-borne non-A. Non-B viral hepatitis genome, Science 244 (1989) 359–362.

[8] M. Houghton, A. Weiner, J. Han, G. Kuo, Q.L. Choo, Molecular biology of the hepatitis C viruses: implications for diagnosis. Development and control of viral disease, Hepatology 14 (1991) 381–388.

[9] T. Suzuki, K. Ishii, H. Aizaki, T. Wakita, Hepatitis C viral life cycle, Adv. Drug Deliv. Rev. 59 (2007) 1200–1212.

[10] V. Lohmann, F. Korner, J.O. Koch, U. Herian, L. Theilmann, R. Bartenschlager, Replication of subgenomic hepatitis C virus RNAs in a hepatoma cell line, Science 285 (1999) 110–113.

[11] T. Wakita, T. Pietschmann, T. Kato, T. Date, M. Miyamoto, Z. Zhao, K. Murthy, A. Habermann, H.G. Krausslich, M. Mizokami, R. Bartenschlager, T.J. Liang, Production of infectious hepatitis C virus in tissue culture from a cloned viral genome, Nat. Med. 11 (2005) 791–796.

[12] M.B. Zeisel, T.F. Baumert, Production of infectious hepatitis C virus in tissue culture: a breakthrough for basic and applied research, J. Hepatol. 44 (2006) 436–439.

[13] R. Bartenschlager, The hepatitis C virus replicon system: from basic research to clinical application, J. Hepatol. 43 (2005) 210–216.

[14] R. Bartenschlager, Hepatitis C virus molecular clones: from cDNA to infectious virus particles in cell culture, Curr. Opin. Microbiol. 9 (2006) 416–422.

[15] V. Brass, D. Moradpour, H.E. Blum, Molecular virology of hepatitis C virus (HCV): 2006 update, Int. J. Med. Sci. 3 (2006) 29–34.

[16] L. Delang, L. Coelmont, J. Neyts, Antiviral therapy for hepatitis C virus: beyond the standard of care, Viruses 2 (2010) 826–866.

[17] C.M. Lange, C. Sarrazin, S. Zeuzem, Specifically targeted anti-viral therapy for hepatitis C – A new era in therapy, Aliment. Pharmacol. Ther. 32 (2010) 14–28.

[18] R.F. Schinazi, L. Bassit, C. Gavegnano, HCV drug discovery aimed at viral eradication, J. Viral Hepat. 17 (2010) 77–90.

[19] T.L. Kieffer, A.D. Kwong, G.R. Picchio, Viral resistance to specifically targeted antiviral therapies for hepatitis C (STAT-Cs), J. Antimicrob. Chemother. 65 (2010) 202–212.

[20] M. Nakamura, A. Aoyama, M.T.A. Salim, M. Okamoto, M. Baba, H. Miyachi, Y. Hashimoto, H. Aoyama, Structural development studies of anti-hepatitis C virus agents with a phenanthridinone skeleton, Bioorg. Med. Chem. 18 (2010) 2402–2411.

[21] H. Aoyama, K. Sugita, M. Nakamura, A. Aoyama, M.T.A. Salim, M. Okamoto, M. Baba, Y. Hashimoto, Fused heterocyclic amido compounds as anti-hepatitis C virus agents, Bioorg. Med. Chem. 19 (2011) 2675–2687.

[22] K. Goto, K. Watashi, T. Murata, T. Hishiki, M. Hijikata, K. Shimotohno, Evaluation of anti-hepatitis C virus effects of cyclophilin inhibitors, cyclosporine A, and NIM811, Biochem. Biophys. Res. Commun. 343 (2006) 879–884.

[23] N. Ishii, K. Watashi, T. Hishiki, K. Goto, D. Inoue, M. Hijikata, T. Wakita, N. Kato, K. Shimotohno, Diverse effects of cyclosporine on hepatitis C virus strain replication, J. Virol. 80 (2006) 4510–4520.

[24] M.P. Windisch, M. Frese, A. Kaul, M. Trippler, V. Lohmann, R. Bartenschlager, Dissecting the interferon-induced inhibition of hepatitis C virus replication by using a novel host cell line, J. Virol. 79 (2005) 13778–13793.

[25] K. Watashi, M. Hijikata, M. Hosaka, M. Yamaji, K. Shimotohno, Cyclosporine A suppresses replication of hepatitis C virus genome in cultured hepatocytes, Hepatology 38 (2003) 1282–1288.

[26] N. Appel, T. Pietschmann, R. Bartenschlager, Mutational analysis of hepatitis C virus nonstructural protein 5A: potential role of differential phosphorylation in RNA replication and identification of a genetically flexible domain, J. Virol. 79 (2005) 3187–3194.

[27] M. Ikeda, M. Yi, K. Li, S.M. Lemon, Selectable subgenomic and genome-length dicistronic RNAs derived from an infectious molecular clone of the HCV-N strain of hepatitis C virus replicate efficiently in cultured Huh7cells, J. Virol. 76 (2002) 2997–3006.

[28] M. Ikeda, K. Abe, H. Dansako, T. Nakamura, K. Naka, N. Kato, Efficient replication of a full-length hepatitis C virus genome, Strain O, in cell culture, and development of a luciferase reporter system, Biochem. Biophys. Res. Commun. 329 (2005) 1350–1359.

[29] M. Yi, S.M. Lemon, Adaptive mutations producing efficient replication of genotype 1a hepatitis C virus RNA in normal Huh7 cells, J. Virol. 78 (2004) 7904–7915.

[30] K.J. Blight, J.A. McKeating, C.M. Rice, Highly permissive cell lines for subgenomic and genomic hepatitis C virus RNA replication, J. Virol. 76 (2002) 13001–13014.

[31] V. Lohmann, S. Hoffmann, U. Herian, F. Penin, R. Bartenschlager, Viral and cellular determinants of hepatitis C virus RNA replication in cell culture, J. Virol. 77 (2003) 3007–3019.

[32] K. Abe, M. Ikeda, H. Dansako, K. Naka, N. Kato, Cell culture-adaptive NS3 mutations required for the robust replication of genome-length hepatitis C virus RNA, Virus Res. 125 (2007) 88–97.

[33] M. Rychlowska, K. Bieńkowska-Szewczyk, Hepatitis C – new developments in the studies of the viral life cycle, Acta Biochim. Pol. 54 (2007) 703–715.

[34] J. Bukh, R.H. Purcell, R.H. Miller, Sequence analysis of the core gene of 14 hepatitis C virus genotypes, Proc. Natl. Acad. Sci. USA 91 (1994) 8239–8243.

[35] O. Ohno, M. Mizokami, R.R. Wu, M.G. Saleh, K. Ohba, E. Orito, M. Mukaide, R. Williams, J.Y. Lau, New hepatitis C virus (HCV) genotyping system that allows for identification of HCV genotypes 1a, 1b, 2a, 2b, 3a, 3b, 4, 5a, and 6a, J. Clin. Microbiol. 35 (1997) 201–207.

[36] T. Kato, T. Date, M. Miyamoto, A. Furusaka, K. Tokushige, M. Mizokami, T. Wakita, Efficient replication of the genotype 2a hepatitis C virus subgenomic replicon, Gastroenterology 125 (2003) 1808–1817.

[37] M. Gao, R.E. Nettles, M. Belema, L.B. Snyder, V.N. Nguyen, R.A. Fridell, M.H. Serrano-Wu, D.R. Langley, J.H. Sun, D.R.I.I. O'Boyle, J.A. Lemm, C. Wang, J.O. Knipe, C. Chien, R.J. Colonno, D.M. Grasela, N.A. Meanwell, L.G. Hamann, Chemical genetics strategy identifies an HCV NS5A inhibitor with a potent clinical effect, Nature 465 (2010) 96–100.

[38] L. Coelmont, S. Kaptein, J. Paeshuyse, I. Vliegen, J.M. Dumont, G. Vuagniaux, J. Neyts, Debio 025, a cyclophilin binding molecule, is highly efficient in clearing hepatitis C virus (HCV) replicon-containing cells when used alone or in combination with specifically targeted antiviral therapy for HCV (STAT-C) inhibitors, Antimicrob. Agents. Chemother. 53 (2009) 967–976.

[39] P. Georgel, C. Schuster, M.B. Zeisel, F. Stoll-Keller, T. Berg, S. Bahram, T.F. Baumert, Virus-host interactions in hepatitis C virus infection: implications for molecular pathogenesis and antiviral strategies, Trends Mol. Med. 16 (2010) 277–286.

[40] T. Suzuki, A Hepatitis C virus-host interaction involved in viral replication: toward the identification of antiviral targets, Jpn. J. Infect. Dis. 63 (2010) 307–311.

[41] W.L. Suarez-Pinzon, J.G. Mabley, R. Power, C. Szabó, A. Rabinovitch, Poly (ADP-ribose) polymerase inhibition prevents spontaneous and recurrent autoimmune diabetes in NOD mice by inducing apoptosis of islet-infiltrating leukocytes, Diabetis 52 (2003) 1683–1688.

[42] S.H. Huang, M. Xiong, X.P. Chen, Z.Y. Xiao, Y.F. Zhao, Z.Y. Huang, PJ34, an inhibitor of PARP-1, Suppresses cell growth and enhances the suppressive effects of cisplatin in liver cancer cells, Oncol. Rep. 20 (2008) 567–572.

[43] G.E. Abdelkarim, K. Gertz, C. Harms, J. Katchanov, U. Dirnagl, C. Szabó, M. Endres, Protective effects of PJ34, a novel, potent inhibitor of poly(ADP-ribose) polymerase (PARP) in vitro and in vivo models of stroke, Int. J. Mol. Med. 7 (2001) 255–260.

[44] S. Patil, S. Kamath, T. Sanchez, N. Neamati, R.F. Schinazi, J.K. Buolamwini, Synthesis and biological evaluation of novel 5(H)-phenanthridin-6-ones, 5(H)-phenanthridin-6-one diketo acid, and polycyclic aromatic diketo acid analogs as new HIV-1 integrase inhibitors, Bioorg. Med. Chem. 15 (2007) 1212–1228.

![PLoS one]

# Genetic Variation of the *IL-28B* Promoter Affecting Gene Expression

Masaya Sugiyama[1,2,5], Yasuhito Tanaka[3], Takaji Wakita[4], Makoto Nakanishi[2], Masashi Mizokami[1]*

1 The Research Center for Hepatitis and Immunology, National Center for Global Health and Medicine, Ichikawa, Chiba, Japan, 2 Department of Biochemistry and Cell Biology, Nagoya City University Graduate School of Medical Sciences, Mizuho, Nagoya, Japan, 3 Department of Virology and Liver Unit, Nagoya City University Graduate School of Medical Sciences, Mizuho, Nagoya, Japan, 4 Department of Virology II, National Institute of Infectious Diseases, Shinjuku, Tokyo, Japan, 5 JSPS Research Fellow, Japan Society for the Promotion of Science, Chiyoda, Tokyo, Japan

## Abstract

The current standard of care for the treatment of chronic hepatitis C is pegylated interferon-α (PEG-IFNα) and ribavirin (RBV). The treatment achieves a sustained viral clearance in only approximately 50% of patients. Recent whole genome association studies revealed that single nucleotide polymorphisms (SNPs) around *IL-28B* have been associated with response to the standard therapy and could predict treatment responses at approximately 80%. However, it is not clear which SNP is most informative because the genomic region containing significant SNPs shows strong linkage disequilibrium. We focused on SNPs in close proximity to the *IL-28B* gene to evaluate the function of each and identify the SNP affecting the *IL-28B* expression level most. The structures of *IL-28A/B* from 5′ to 3′-UTR were determined by complete cDNA cloning. Both *IL-28A* and *28B* genes consisted of 6 exons, differing from the CCDS data of NCBI. Two intron SNPs and a nonsynonymous SNP did not affect *IL-28B* gene function and expression levels but a SNP located in the proximal promoter region influenced gene expression. A (TA) dinucleotide repeat, rs72258881, located in the promoter region was discovered by our functional studies of the proximal SNPs upstream of *IL-28B*; the transcriptional activity of the promoter increased gradually in a (TA)$_n$ length-dependent manner following IFN-α and lipopolysaccharide stimulation. Healthy Japanese donors exhibited a broad range of (TA) dinucleotide repeat numbers from 10 to 18 and the most prevalent genotype was 12/12 (75%), differing from the database (13/13). However, genetic variation of *IL-28A* corresponding to that of *IL-28B* was not detected in these Japanese donors. These findings suggest that the dinucleotide repeat could be associated with the transcriptional activity of *IL-28B* as well as being a marker to improve the prediction of the response to interferon-based hepatitis C virus treatment.

## Introduction

A novel group of cytokines was discovered simultaneously by two independent groups in 2003 and named interferon lambda (IFN-λ) [1,2] or type III IFN. Type III IFN comprises three members, IFN-λ1, 2, and 3 or *IL-29* and *IL-28A*, and *IL-28B*, respectively. Type III IFN is a member of the class II cytokine family. This family includes type I, II, and III interferons and the IL-10 family (IL-10, IL-19, IL20, IL-22, IL-24, and IL-26). IFN-λ uses a distinct receptor complex consisting of a unique subunit, named IFN-λR1, and the IL-10R2 subunit. Expression of the IFN-λR1 receptor subunit is highly restricted, whereas the type I IFN receptor complex and the IL-10R2 receptor were detected in most cell types [1,2,3,4,5,6]. The IL-10R2 receptor subunit is shared by IL-10, IL-22, IL-24, IL-26, and IFN-λ. This suggests that type III IFNs act in a rather cell-type specific manner to mediate their biological functions. Type III IFNs trigger a type I IFN-like gene expression profile [5,6,7], which has been shown to have antiviral activity *in vitro* and *in vivo* [1,2,5,6,8]. Thus, the two types of IFN seem to have similar biological effects at a cellular level. IFN-α and IL-29/28A treatment reduced the concentration

of hepatitis C virus (HCV) plus-strand RNA in an *in vitro* assay [6,9,10,11]. In addition, IL-29 may have therapeutic value against chronic viral hepatitis in human patients [5].

Recently, a genome-wide association study (GWAS) revealed that several highly correlated common single nucleotide polymorphisms (SNPs), in a linkage disequilibrium (LD) block encompassing the *IL-28B* genes on chromosome 19q13, are implicated in the response of chronic hepatitis C (CHC) patients to pegylated IFN-alpha (PEG-IFNα) and ribavirin (RBV) [12,13,14]. The CC genotype of rs12979860 and TT genotype of rs8099917 are associated in CHC patients with a sustained viral response (SVR) of 2.5 or greater rate, which is dependent of ethnicity, compared to the other genotypes. Moreover, the CC genotype of rs12979860 and TT genotype of rs8099917 favor spontaneous clearance of HCV [15].

We have reported the genomic analysis of approximately 15 kb containing the significant SNPs using Haploview software for LD and haplotype structure [14,16]. To analyze the difference in LD pattern between races, we performed LD mapping with these SNPs on JPT (Japanese in Tokyo), CEU (Utah residents with ancestry from Northern and Western Europe) or YRI (Yoruba in

Ibada, Nigeria) populations. These SNPs were in strong LD in JPT and CEU populations, although relatively low LD was predicted in the YRI population [14,16], suggesting that any of the SNPs located in this region could be responsible for treatment response. Because of the strong LD, tests for independence among these variants were not able to reveal which of these SNPs is uniquely responsible for the association with virological response (VR) or non-virological response (NVR). The identification of the primary genetic variant located in the LD block remained critical, although the risk haplotype tended to influence the expression levels or activity of *IL-28B* [13,14]. In this study, we sought to determine the primary SNP affecting IL-28B expression and/or its function by focusing on the proximal regulatory region of *IL-28B*.

*IL-28B* was discovered as a member of the IFN-λ family by Sheppard et al. and Kotenko et al. [1,2]. They discovered this family, *IL-29, IL-28A*, and *IL-28B* and the specific receptor, *IL-28R1*, by applying individual computational techniques to the draft human genome. However, the start codon of IFN-λ differs between the reports, with an additional 12 nucleotides at the N-terminus in all IFN-λs reported by Sheppard et al. (Fig. S1). The sequence similarity between these ORFs is approximately 96.7% and, especially, there is a high degree of identity between *IL-28A* and *IL-28B* cDNA (approximately 98%). Figure 1A shows the locations of *IL-28A/B* gene, the significant SNPs around *IL-28B* related to anti-HCV therapy reported in previous studies [12,13,14], and $(TA)_n$ repeats in the regulatory region of *IL-28A* and *B*. The SNPs information assessed in this study is summarized in Table 1 and the locations of the SNPs are shown in the schematic of the *IL-28B* gene (Fig. 1B). The reference sequences of *IL-28A* or *IL-28B* cDNA, registered in NCBI CCDS, are composed of 6 exons and 5 exons, respectively (Fig. 1B). Because high sequence similarity was observed between *IL-28A* and *IL-28B* from CpG to the region downstream of 3'-UTR (Fig. S2), the genes were almost completely identical around transcription start

site (TSS) (>99%). Then, we determined the likely gene structure using a complete cDNA cloning method because a similar transcriptional mechanism was expected for *IL-28A* and *IL-28B*.

## Materials and Methods

### Genome samples

Genome samples were obtained from 20 healthy volunteers (HV). Peripheral blood mononuclear cells (PBMC) collected from HV were isolated using the BD Vacutainer CPT Method (BD Biosciences). Genomic DNAs were extracted by standard methods. SNPs were selected from the database at GWAS database (https://gwas.lifesciencedb.jp/cgi-bin/gwasdb/gwas_top.cgi). Written informed consent was provided by all participants in the genotyping study following procedures approved by the Ethical Committee at Nagoya City University.

### Cell lines

Human hepatocellular carcinoma cell lines, HepG2 and HuH7, human hepatocyte cell lines, HuSE2 (kindly provided by Dr. Hijikata in Kyoto University), and the human cervical cancer cell line, HeLa (obtained from The American Type Culture Collection), were cultured in Dulbecco's modified Eagle's medium supplemented with 10% (v/v) fetal bovine serum, 100 U ml$^{-1}$ penicillin and 100 mg ml$^{-1}$ streptomycin. Human leukemia virus type 1 transformed cell line, MT-2 (a gift from Dr. Ueda in Nagoya City University), Burkitt lymphoma cell line, Raji, and human T cell leukemia cell line, Jurkat (obtained from The American Type Culture Collection), were cultured in RPMI 1640 medium supplemented with 10% (v/v) fetal bovine serum, 100 U ml$^{-1}$ penicillin and 100 mg ml$^{-1}$ streptomycin. All incubations were performed at 37°C in a 5% $CO_2$ gassed incubator. Recombinant human IFN-λ2 and -3 were purchased from R&D Systems (Abingdon, UK). Natural human IFN-α was
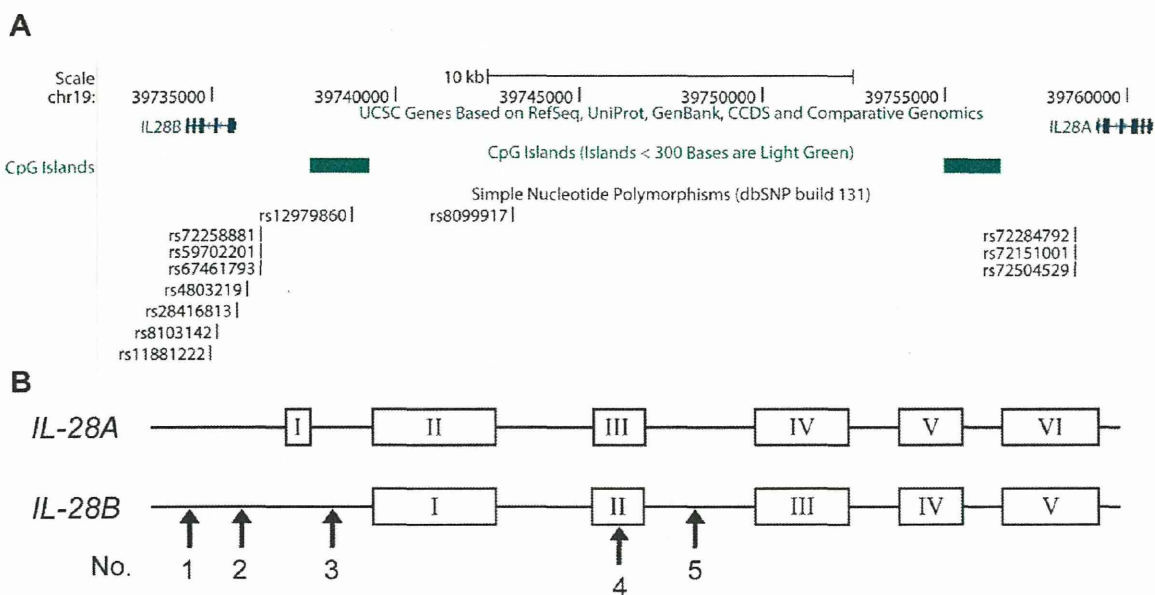


**Figure 1. The position of significant SNPs and *IL-28A/B* in chromosome 19, retrieved from the database.** (A) The *IL-28A/B* genes located in chromosome 19q13 are described in the genome map of the UCSC genome browser. The significant proximal SNPs around *IL-28B* associated with response to PEG-IFN/RBV therapy are shown in the map [14]. SNPs of $(TA)_n$ variation at the regulatory region of *IL-28A* are displayed in the position corresponding to that of *IL-28B*, which is not associated with anti-HCV therapy. (B) The schematic of *IL-28A/B* gene structure is described based NCBI CCDS data. Arrows show five significant SNPs examined in this study (see Table 1).
doi:10.1371/journal.pone.0026620.g001

- 1351 -

**Table 1.** Significant SNPs around *IL-28B*.

| Feature | rs ID | Allele 1/2*[1] | Minus strand*[2] | Location | No. |
|---|---|---|---|---|---|
| DIP*[3] | rs72258881*[4] | ATAT/- | TATA/- | Regulatory | 1 |
| Substitution | rs4803219 | C/T | G/A | Regulatory | 2 |
| | rs28416813 | C/G | G/C | Intron | 3 |
| | rs8103142 | T/C | A/G | Nonsynonymous | 4 |
| | rs11881222 | A/G | T/C | Intron | 5 |

*[1]These data were derived from dbSNP. Allele 2 is the risk allele of HCV therapy reported by Tanaka et al., except for rs72258881.
*[2]Complementary nucleotides are shown because *IL-28B* is coded on the minus strand.
*[3]DIP: deletion/insertion polymorphism.
*[4]The ID represents rs72258881, rs59702201, and rs67461793 because these three are located in the same genomic region, the TA repeat.
doi:10.1371/journal.pone.0026620.t001

purchased from Hayashibara co. ltd. (Okayama, Japan). The mRNA expression levels of receptors stimulated in this study were confirmed by PCR using gene specific primer (Table S1 and Fig. S3),

## Plasmid Construction

As a T/G heterozygote genome of rs8099917 with a strong LD was used as the PCR template, amplicons from the major and minor alleles were obtained for the assay described below. PCR was carried out to amplify the fragment from −858 nt of the ATG site to TGA of *IL-28B*, and the products were inserted into pcDNA3.1/Hyg (pcDNA/MA or mi) or pcDNA3.1/Hyg vector deleting CMV promoter (pdCMV/MA or mi). A FLAG sequence was conjugated to 6th exon, removing the stop codon, for real time PCR analysis. The promoter region from nucleotide position −858 to +30 of *IL-28B* was amplified using pdCMV/MA or mi vector and inserted into pGL4 vector for the luciferase assay. A vector with an antisense insert was prepared as a control. For expression constructs, the wild type (WT) plasmids, pcDNA3.1/wild expressing human IL-28B, and pcDNA3.1/ns-mut expressing human IL-28B harboring a K$^{74}$R mutation, were generated using pcDNA3.1/V5-His-TOPO® (Invitrogen, San Diego, CA) and were used in the subsequent transfections. In addition, pcDNA3.1/AS expressing antisense strand of IL-28B was constructed as a control. We also obtained a pISRE-luc plasmid (provided by Sakamoto N., Tokyo Medical Dental University, Tokyo, Japan). The pGL4.74 vector encoding Renilla Luciferase was purchased from Promega (Madison, WI). These primer sequences are available on request. The above expression vectors were modified for the analysis of splicing function by introducing two intron SNPs (rs28416813 and rs11881222) (Table 1), which were pcDNA/WT, d-iSNPs.

## Transient transfections

Transient transfections of HeLa, Jurkat, Raji, HuH7, HepG2, or HuSE2 (hepatocellular carcinomas cell line) cells were carried out using FuGene HD (Roche) or the Cell Line Nucleofector kit (Amaxa Biosystems) according to the manufacturers' protocols. Briefly, Cells ($2 \times 10^5$) were seeded into a 6 well plate and transfected with for FuGene HD. For the electroporation method, cells ($1.0 \times 10^6$) were collected and resuspended in Nucleofector solution V for each individual transfection sample.

## 5'-, 3'-RACE based on full-length cDNA cloning

Total RNA was prepared from cell lines stimulated with lipopolysaccharide (LPS) (0127:B8, Sigma-Aldrich) for 4 hours

after 100 U/mL of IFN-α for 16 hours by following previous paper [17]. A GeneRacer Kit (Invitrogen Life Technologies) was used to obtain the complete cDNA sequence of *IL-28A/B* following manufacturer's instructions. Briefly, the GeneRacer RNA Oligo was ligated to the 5' end specifically of full-length mRNA within the total RNA mixture. This ligated mRNA was then converted to cDNA using reverse transcriptase (RT) and the GeneRacer Oligo dT Primer. Next, this cDNA was used for PCR using the oligonucleotides of GeneRacer 5' Primer and P1 primer which hybridized to the coding strand of the *IL28A/B* (Table S1). The resulting PCR products were then used for a second round of PCR using the oligonucleotides GeneRacer 5' Nested Primer, which represents the DNA equivalent of the 3' end of the GeneRacer RNA Oligo, and P2, which hybridizes to the coding strand of the *IL-28A/B* 5' to the P1 hybridization site. For 3' RACE, the cDNA was subjected to the polymerase chain reaction (PCR) to amplify the 3' end using a forward gene-specific primer P3 designed from *IL-28A/B* and the GeneRacer 3' primer provided with the kit. Nested PCR, using the same gene-specific primer and GeneRacer 3' nested primer, was performed. The PCR product of 5' and 3' RACE was cloned into pCR4-TOPO TA vector according to the manufacturer's instructions (Invitrogen). Ten clones were isolated and subjected to automated sequencing (ABI3100, ABI) in our core facility.

## Protein expression and purification

Recombinant IL-28B and its mutant were produced by transfecting Free-Style™ 293-F cells (purchased from Invitrogen, Carlsbad, CA) with the expression plasmid, which was grown in 5000 ml of FreeStyle 293 Expression Medium, following the manufacturer's recommendations (Invitrogen, Carlsbad, CA). Cultures were maintained at >90% viability on a shaker plate (Titer Plate Shaker; Lab-Line Instruments, Melrose Park, NJ) moving at 125 rpm in a 37°C incubator with 8% $CO_2$ and subculturing at a 1:10 ratio upon reaching a density of $2 \times 10^6$ cells per ml. Cell density and viability were evaluated with a hemocytometer using 0.4% trypan blue staining. After 96 h, the transfected cell culture was harvested. The supernatant containing the secreted recombinant protein was centrifuged ($100 \times g$, 15 min), frozen, and stored at −30°C until use. The 293-F cells supernatant containing the recombinant protein was loaded onto a $Ni^{2+}$ column (Amersham Biosciences) following the manufacturer's directions. Fractions were eluted with 80, 100, 250, and 1000 mM imidazole (in 50 mM Tris, 300 mM NaCl, pH 8.0), and the fraction eluted at 250 mM was pooled and concentrated in an Amicon (10 kDa molecular weight cutoff) to 1 ml (Amersham Biosciences).

## Western blot analyses

Purified recombinant protein was loaded onto 12% sodium dodecyl sulfate gels. Proteins were detected with goat anti-IL28 (1:2000) polyclonal antibody (Santa Cruz Biotechnology, Santa Cruz, CA) and the secondary antibody. Proteins were visualized using ECL Plus Western blotting detection reagents (GE Healthcare) and a LuminoImager (LAS-3000; Fujifilm). The band densities were analyzed with the Multi Gauge software (version 3.1; Fujifilm).

## IL-28A/B promoter genotyping

Germ-line DNA was extracted from PBMC according to standard methods [14]. Twenty HV samples were genotyped for the dinucleotide insertion/deletion (indel) present in the promoter region of *IL-28A* or *B*, as described below. Twenty ng of genomic DNA were subjected to PCR analysis in 50 μl aliquots containing

**A**

5' RACE          3' RACE

M   NC   HeLa      M   NC   HeLa

**B**

```
IL-28A    1 ------------------------------------------------------------    1
IL-28B    1 ------------------------------------------------------------    1
5RACE-A   1 GAATTACATCCCAGACAGAGCTCAAAACTGACAGAAAGAGTCAAAGCCAGGACACAGTCT   60
5RACE-B   1 GAATTACATCCCAGACAGAGCTCAAAACTGACAGAAAGAGTCAAAGCCAGGACACAGTCT   60

IL-28A    1 ------------------------------------------------------------    1
IL-28B    1 ------------------------------------------------------------    1
5RACE-A  61 GAGATCCAGAAGAGGGGACTGAAAAGAACAGAGACTCCAGACAAGACCCAAACAGACCCT  120
5RACE-B  61 GAGATCCAGAAGAGGGGACTGAAAAGAACAGAGACTCCAGACAAGACCCAAACAGACCCT  120

IL-28A    1 ----------------------------------------------------ATGAAACTA    9
IL-28B    1 ------------------------------------------------------------    1
5RACE-A 121 GGGTGACAGCCTCAGAGTGTTTCTTCTGCTGACAAAGACCAGAGATCAGGA.........  180
5RACE-B 121 GGGTGACAGCCTCAGAGTGTTTCTTCTGCTGACAAAGACCAGAGATCAGGA.........  180

IL-28A   10 GACATGACTGGGGACTGCACGCCAGTGCTGGTGCTGATGGCCGCAGTGCTGACCGTGACT   69
IL-28B    1 ---...C.........T..........................................   57
5RACE-A 181 ........C.........T..........................................  240
5RACE-B 181 ........C.........T..........................................  240

IL-28A   70 GGAGCAGTTCCTGTCGCCAGGCTCCACGGGGCTCTCCCGGATGCAAGGGGCTGCCACATA  129
IL-28B   58 ....................................G.......................  117
5RACE-A 241 ....................................G.......................  300
5RACE-B 241 ....................................G.......................  300

IL-28A  130 GCCCAGTTCAAGTCCCTGTCTCCACAGGAGCTGCAGGCCTTTAAGAGGGCCAAAGATGCC  189
IL-28B  118 ............................................................  177
5RACE-A 301 ............................................................  357
5RACE-B 301 ............................................................  357
```

**C**

```
IL-28A  421 TCAGCCCACGGCAGGGCCCAGGACCCGGGGCCGCCTCCACCATTGGCTGTACCGGCTCCA  480
IL-28B  421 .....................................................C......  480
3RACE-A   1 ------------------------------------------...............  15
3RACE-B   1 ------------------------------------------...C...........  15

IL-28A  481 GGAGGCCCCAAAAAGGAGTCCCCTGGCTGCCTCGAGGCCTCTGTCACCTTCAACCTCTT  540
IL-28B  481 ............................................................  540
3RACE-A  16 ............................................................   75
3RACE-B  16 ............................................................   75

IL-28A  541 CCGCCTCCTCACGCGAGACCTGAATTGTGTTGCCAGTGGGGACCTGTGTGTCTGACCCTC  600
IL-28B  541 ................................................C..........T  600
3RACE-A  16 ............................................................   75
3RACE-B  16 ................................................C..........T   75

IL-28A  601 CCACCAGTCATGCAACCTGAGATTTTATTTATAAAATTAGCCACTTGTCTTAATTTATTGC  660
IL-28B  601 ..G.......................................G............T  660
3RACE-A  16 ............................................................   75
3RACE-B  16 ..G.......................................G............T   75

IL-28A  661 CACCCAGTCGCTATTTATGTATTTGTGTGTCTAAATCCAACTCACCTCCAGGAAAATGTT  720
IL-28B  661 ...................A........................................  720
3RACE-A  16 ............................................................   75
3RACE-B  16 ...................A........................................   75

IL-28A  721 TATTTTTCTACTTTTTATAACCCTTGTTGAATAAACAA--AGGAAAAGACACTCATGAC  780
IL-28B  721 .................GA..T...............TG...........C......  780
3RACE-A 256 .................GA..T...........--..........AAAAAAA  308
3RACE-B 256 .....................TG...........AAAAAAA  308
                                      polyA signal          polyA tail
```

**D**



TSS

IL-28B

No.    1   2   3        4   5

**Figure 2. The determination of *IL-28B* gene structure and UTR region.** *IL-28A/B* cDNA was isolated using a complete cDNA cloning method and the entire sequences were determined using HeLa, MT-2, and Raji cell lines and PBMC from healthy volunteers. (A) 5'- and 3'-RACE analyses were used to determine the complete sequence of *IL-28A/B* mRNA after LPS stimulation (3 µg/mL) for 4 h following IFN-α treatment (100 U/mL) for 16 h. A representative example of agarose gel electrophoresis is shown for the non-stimulated control (NC). PCR products were inserted into the cloning vector and 6 clones of 5'- and 3'-RACE were analyzed by sequencing. (B) mRNA sequences of the 5' terminal region were aligned using CCDS retrieved from NCBI and RACE data of *IL-28A/B*. The upper two sequences are reference sequences from the NCBI CCDS and the lower two are representative sequences of *IL-28A* and *28B* obtained from 5'-RACE. The underlined triplet indicates the start codon of each gene and arrow shows the splice junctions. (C) mRNA sequences of the 3' terminal region were aligned using CCDS retrieved from NCBI and RACE data from *IL-28A/B*. The double-underlined triplet indicates the stop codon of each gene and arrows show the splice junctions. The polyA signal and representative site of polyadenylation also are shown. (D) The derived gene structure of the *IL-28B* is shown with the significant SNPs. The location of SNP No. 3 was changed from the regulatory to an intron region. The transcription start site (TSS) is found behind SNP No. 2.
doi:10.1371/journal.pone.0026620.g002

20 pmol of each primer, 5×PrimeSTAR GXL Buffer, 2.5 mM each deoxynucleotide triphosphates, and 1.25 units of PrimeStar GXL DNA polymerase (TAKARA Bio Inc, Tokyo, Japan). The primer pair, G1 and G2 (listed in Table S1), was used for the simultaneous amplification of the *IL-28A* and *28B* regulatory regions. The PCR conditions were as follows: 30 cycles of 10 s at 98°C, and 120 s at 68°C in addition of initial denaturation at 98°C for 5 min and a final extension at 68°C for 10 min. To separate the *IL-28A* amplicon from that of *IL-28B*, 10 µl of PCR products were analyzed using agarose gel electrophoresis and extracted with QIAquick Gel Extraction Kit (Qiagen). Each extracted product was analyzed by direct sequencing using Seq1 and Seq2 primers (Table S1). For further testing of the TA repeat, heterozygous samples were cloned into the pGEM-Teasy vector to count the number of TA repeats in each allele. Six clones were isolated and subjected to sequencing analysis using the primers described above.

### Reporter assay

Luciferase assays of recombinant protein were performed using Dual-Glo Luciferase reporter assay system (Promega, Fitchburg, WI). In toll-like receptor (TLR)-stimulated experiments Raji cells were transfected and left for 16 h with 100 U/mL of IFN-α, then were exposed to LPS (3 µg/ml) for 4 h before harvesting. For assessments of recombinant protein, HeLa cells were transfected with pISRE-Luc and pGL4.74, and were harvested 24 h after IFN-α or λ treatment. The chemiluminescence was measured by SpectraMax L (Molecular Devices, Sunnyvale, CA). Firefly luciferase activity was normalized to Renilla activity to adjust for transfection efficiency.

### Real-time PCR detection

Jurkat cells were transfected with the *IL-28B* expression vector harboring a FLAG sequence derived from the natural promoter (pdCMV/MA, mi, or AS). To induce IL-28B expression, TLR and IFN-α stimulation was given as described above. FLAG and glyceraldehyde-3-phosphate dehydrogenase (GAPDH) mRNA expression were measured using a real-time PCR performed on ABI Prism 7700 sequence detection system (Applied Biosystems) using primer sets (Table S1) after total RNA extraction and reverse transcription (RT) using an RT kit and TaqMan Universal PCR master mix (both Applied Biosystems), according to the manufacturer's manual. Relative gene expression was calculated as a fold induction compared to the control. Data were analyzed by the 2[-Delta Delta C(t)] method using Sequence Detector version 1.7 software (Applied Biosystems) [18] and were normalized using human GAPDH. A standard curve was prepared by serial 10-fold dilutions of human cDNA or FLAG plasmid. The curve was linear over 7 logs with a 0.998 correlation coefficient.

### Statistical Analysis

Statistical analyses were conducted by using SPSS software package (SPSS 18J, SPSS, Chicago, IL) and Microsoft Excel 2007

(Microsoft co., Redmond, WA). Discrete variables were evaluated by Fisher's exact probability test. The P values were calculated by two-tailed student's t-tests for continuous data and chi-square test for categorical data, and those of less than 0.05 were considered as statistically significant.
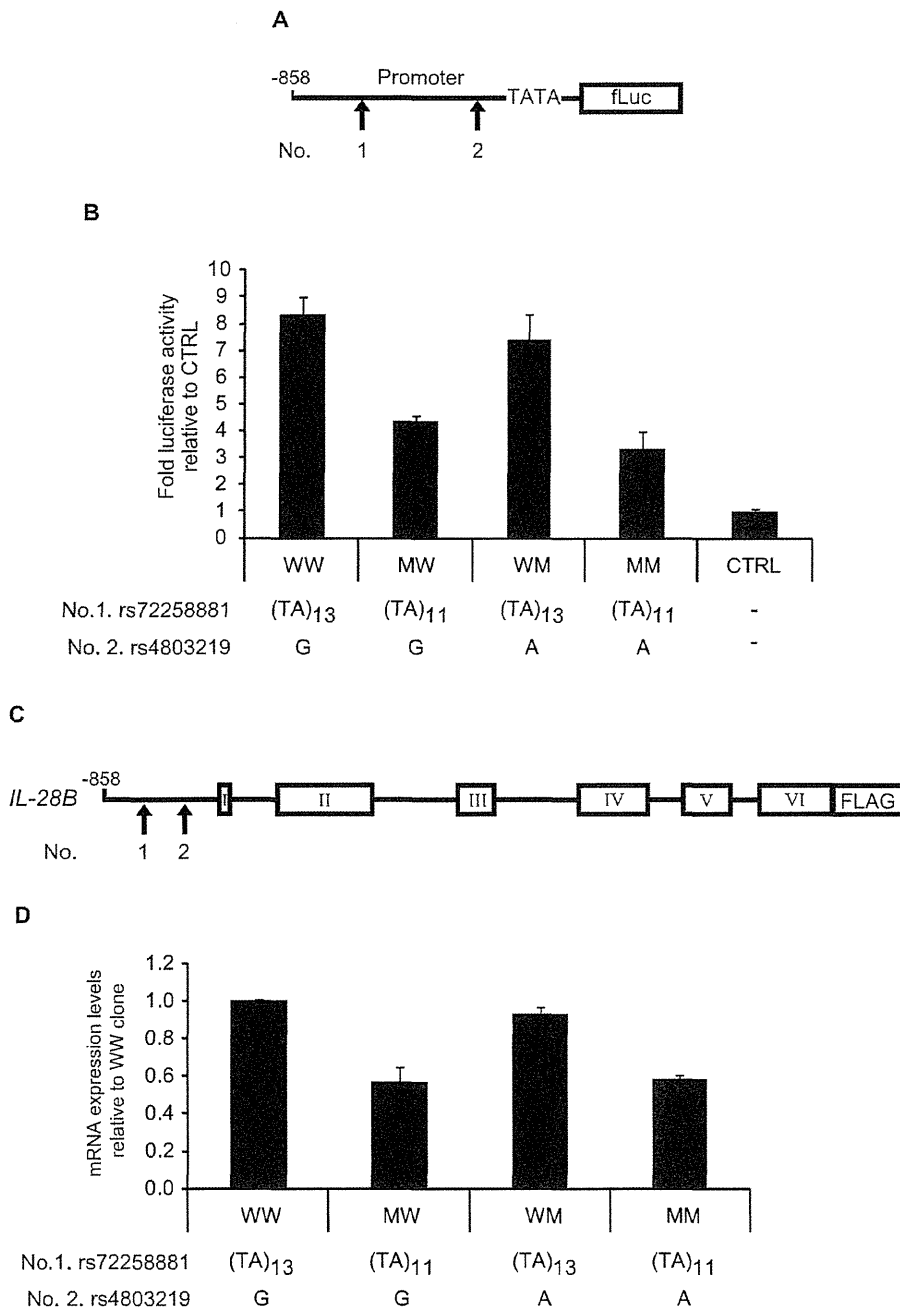
## Results

### The identification of IL-28B gene structure

To define the human *IL-28A* or *IL-28B* gene structure, 5'-RACE and 3'-RACE were performed on total extracted RNA from HeLa, MT-2, Raji, HuH7 cells, and PBMCs from healthy volunteers (Fig. 2A). The sequences obtained matched the genomic contig of AC011445, which contains the sequence of *IL-28A* and *IL-28B* in forward and reverse orientations, respectively. All intron/exon junctions conformed to the canonical GT-AG rule. After stimulation of cells with LPS (3 µg/ml) for 4 h following IFN-α treatment (100 U/mL) for 16 h, *IL-28A/B* transcripts were detected in RACE experiments, but these were not detected in unstimulated cells. The representative TSSs are shown in Fig. 2B and showed little variation among cloned mRNA transcripts. The same 3'-UTR fragment also was detected without any intron in the 3'-RACE experiments (Fig. 2C). A polyadenylation signal (AAAUAAA), located in the 3'-UTR, was found upstream of the polyadenylation site in all samples. All sequences from the transcripts were aligned on the 5'-UTR, the six exons, and the 3'-UTR region of *IL-28A/B*. No different mRNA transcripts of *IL-28A/B* were found in our experiment. Taken together, the *IL-28B* gene structure comprised six exons (see Fig. 2D), and the location of SNP no. 3 (rs28416813) is in an intron, rather than a regulatory region (Table 1).

### The effect of regulatory SNPs on promoter activity

Because the TSS was upstream of the position described in previous reports (Fig. 2), two rSNPs (rs72258881 and rs4803219) in the regulatory region were more specifically located in the TSS. A luciferase reporter approach was used to assess the effects of the two rSNPs on promoter activity. Luciferase vectors harboring the rSNPs were constructed and used for transfections (Fig. 3A). The promoter activities of the constructs were measured after stimulation with LPS (3 µg/ml) for 4 h following IFN-α treatment (100 U/mL) for 16 h. The transcriptional activity of constructions harboring the (TA)₁₁ mutation was reduced (Fig. 3B). Substitution in the rSNP (rs4803219) showed little effect on the transcriptional activity, whereas the number of TA repeats could be responsible for the putative region controlling basal transcription. To confirm the transcriptional activity, Jurkat cells were transfected with full length constructs expressing the FLAG sequence under the control of the natural promoter (Fig. 3C). To avoid the detection of endogenous mRNA, the mRNA with the FLAG sequence was specifically detected by real time PCR using the FLAG primer. The constructs harboring (TA)₁₁ yielded lower expression levels

- 1354 -

**A**



**B**



|                      |           |           |           |           |      |
| -------------------- | --------- | --------- | --------- | --------- | ---- |
| No.1. rs72258881     | $(TA)_{13}$ | $(TA)_{11}$ | $(TA)_{13}$ | $(TA)_{11}$ | -    |
| No. 2. rs4803219     | G         | G         | A         | A         | -    |

**C**



**D**



|                      |           |           |           |           |
| -------------------- | --------- | --------- | --------- | --------- |
| No.1. rs72258881     | $(TA)_{13}$ | $(TA)_{11}$ | $(TA)_{13}$ | $(TA)_{11}$ |
| No. 2. rs4803219     | G         | G         | A         | A         |

**Figure 3. Transcriptional activity of the *IL-28B* promoter region compared between major and minor alleles.** (A) The pGL4 reporter plasmid was constructed by subcloning the *IL-28B* promoter subfragment (nt −858 to +30). The combinations of two regulatory SNPs (rs72258881 or rs4803219) were introduced into the pGL4 vector (pGL4/WW, MW, WM, and MM). (B) Raji cells were co-transfected with pGL4 plasmids (0.05 g), and pGL4.74 control plasmid (0.05 g), and tested for firefly as well as renilla luciferase after LPS stimulation (3 μg/mL) for 4 h following IFN-α treatment (100 U/mL) for 16 h. These cells were seeded in a 96-well plate at $10^4$ cells/well. The luciferase activities were normalized with renilla activities and data are presented as fold induction from activation of control vector. Bars indicate the means ± SD of triplicate determinations and the results are from one of three experiments. Statistical analyses are shown in table S2 to avoid complication. (C) For real-time PCR, the combinations of two regulatory SNPs (rs72258881 or rs4803219) were introduced into the pdCMV vector harboring a FLAG sequence (pdCMV/WW, MW, WM, and MM). (D) Jurkat cells were co-transfected with pdCMV plasmids (0.05 μg) and secreted alkaline phosphatase (SEAP) control plasmid (0.05 μg) and the expression levels were quantified using specific primer after LPS and IFN-α stimulation. The FLAG expression levels were normalized with SEAP activities and GAPDH as described in method section. Data are presented as fold induction from expression levels of pdCMV/WW. Bars indicate the means ± SD of triplicate determinations and the results are from one of three experiments. Statistical analyses are shown in table S3 to avoid complication.
doi:10.1371/journal.pone.0026620.g003

after IFN-α and LPS stimulation (Fig. 3D), suggesting that the length of TA repeat in the regulatory region of *IL-28B* could affect the regulation of *IL-28B* transcription.

## Two intron SNPs located near the branch site of splicing

To determine the effect of the two iSNPs on pre-mRNA splicing, HeLa cells were transfected with wild type (WT), a construct with a double mutation of the iSNPs (d-iSNPs), or an antisense (AS) plasmid driven by the CMV promoter (Fig. 4A). The construct providing antisense transcription controlled by the CMV promoter was used to control for splicing defects (AS). Transcripts were analyzed by RT-PCR using primers in exon 1-2, 3-4, and 4-5. The RNA isolated from the WT and d-iSNPs yielded a single band using the three primer pairs. In contrast, longer amplicons were generated in cells expressing the antisense construct (Fig. 4B). The PCR products were sequenced to confirm the origin of the aberrant splicing events derived from the antisense construct (data not shown). The sequence analyses confirmed that PCR products from the WT and d-iSNPs were generated by normal splicing, suggesting that these two intron SNPs resulted in no splicing defects under these conditions.

## No effect of nonsynonymous SNPs on IL-28B function

A nonsynonymous SNPs (rs8103142) located in the $3^{rd}$ exon (Table 1 and Fig. 2D) led to the amino acid substitution $K^{74}R$ (Fig. 5A). Interestingly, the amino acid at this position is almost always arginine in homologous mammalian IFN-λs (e.g. human IL-28A, mouse IL-28A/B, and rhesus IL-28A/B). Then, the $K^{74}R$ substitution was expected to change IL-28B activity. The purified recombinant IL-28B protein (wild type) and the variant (ns-mut) were recognized by anti-IL-28B polyclonal antibody in a western blot assay (Fig. 5B). Based on spectrophotometric measurement of the protein concentration of the eluted fraction, it was calculated that at least 360 μg/mL of purified recombinant IL-28B protein (wild type and ns-mut) was obtained after purification. Flow-through liquid without recombinant protein was provided in the column preparing the sample of pcDNA3.1/AS (Fig. 5B). Molecular processing of IL-28B protein was confirmed to

determine the precise N-terminal amino acid by peptide sequencer as the processing site of signal peptide was predicted by computer simulation (http://www.uniprot.org/uniprot/Q8IZI9). Then, the N-terminal sequence, VPVAR, was obtained (data not shown), suggesting that the simulation data was consistent with the form of physiological protein.

To evaluate the effect of nsSNPs on ISRE activity, three hepatoma cell lines (HuH7, HepG2, and HuSE2) expressing IL-28R1 and IL-10R2 were transfected with pISRE-Luc and pGL4.74. These recombinant proteins were added to the supernatant (5 ng/mL each). As shown in Fig. 5C, ISRE activity of the ns-mut protein was similar to that of wild type protein in each cell line. IFN-α (100 U/mL), as a positive control of ISRE activity, showed a strong ISRE activity. These results suggested that the nonsynonymous mutation of rs8103142 did not affect IL-28B activity *in vitro*.

## The genetic variation of TA repeats at the upstream of *IL-28B*

The reference sequence (RefSeq) of the human genome in the international database registers the TA repeat SNPs, rs72284729 or rs72258881, in the regulatory regions of *IL-28A* and *IL-28B*, respectively. The registered basal number of $(TA)_n$ is 8 in the regulatory region of *IL-28A* on the plus strand, whereas that of *IL-28B* is 13 on the minus strand encoding the gene (Table 2). From 20 Japanese healthy volunteers, genomic DNA was extracted to determine the actual $(TA)_n$ number located in the region of *IL-28A* or *IL-28B* by direct sequencing and, when direct sequencing chromatographs of $(TA)_n$ heterozygotes showed mixed patterns from the end of the TA repeat (Fig. S4), the mixed samples were subjected to cloning analysis. Interestingly, the $(TA)_n$ number in *IL-28A* was consistently different from dbSNP data, whereas that of *IL-28B* showed varying numbers along with SNPs data. The $(TA)_n$ range of *IL-28B* was from 10 to 18, and the most prevalent genotype was 12/12 (75%) in healthy Japanese volunteers.

To determine the functional significance of the TA indel, the regulatory region from −858 bp to +30 bp modifying the $(TA)_n$ number was cloned into the pGL4 reporter vector, transfected into HeLa cells, and assessed for firefly luciferase reporter gene
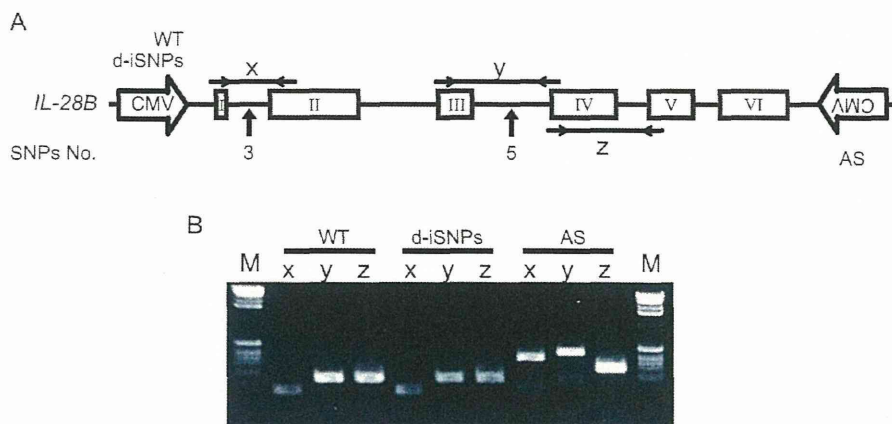


**Figure 4. The determination of intron SNPs located near the branch site of splicing.** (A) The expression plasmid of WT, d-iSNPs, or antisense (AS) derived from the CMV promoter was transfected into HeLa cells. Schematic of the WT, d-iSNPs, or AS used in the transfection experiments. PCR primers were designed to amplify products between exons. The effect of No. 3 and 5 SNPs (rs28416813 or rs11881222) on splicing were examined by amplicons x and y, respectively. The amplicon z was used for a splicing control. (B) Isolated RNAs were amplified by RT-PCR. The amplified products were checked by 2% agarose gel electrophoresis. The bands from the AS plasmid transcribing antisense represented abnormal splicing of mRNA as a control. Results shown are representative of three independent experiments.
doi:10.1371/journal.pone.0026620.g004

− 1356 −

**A**



**B**



**C**
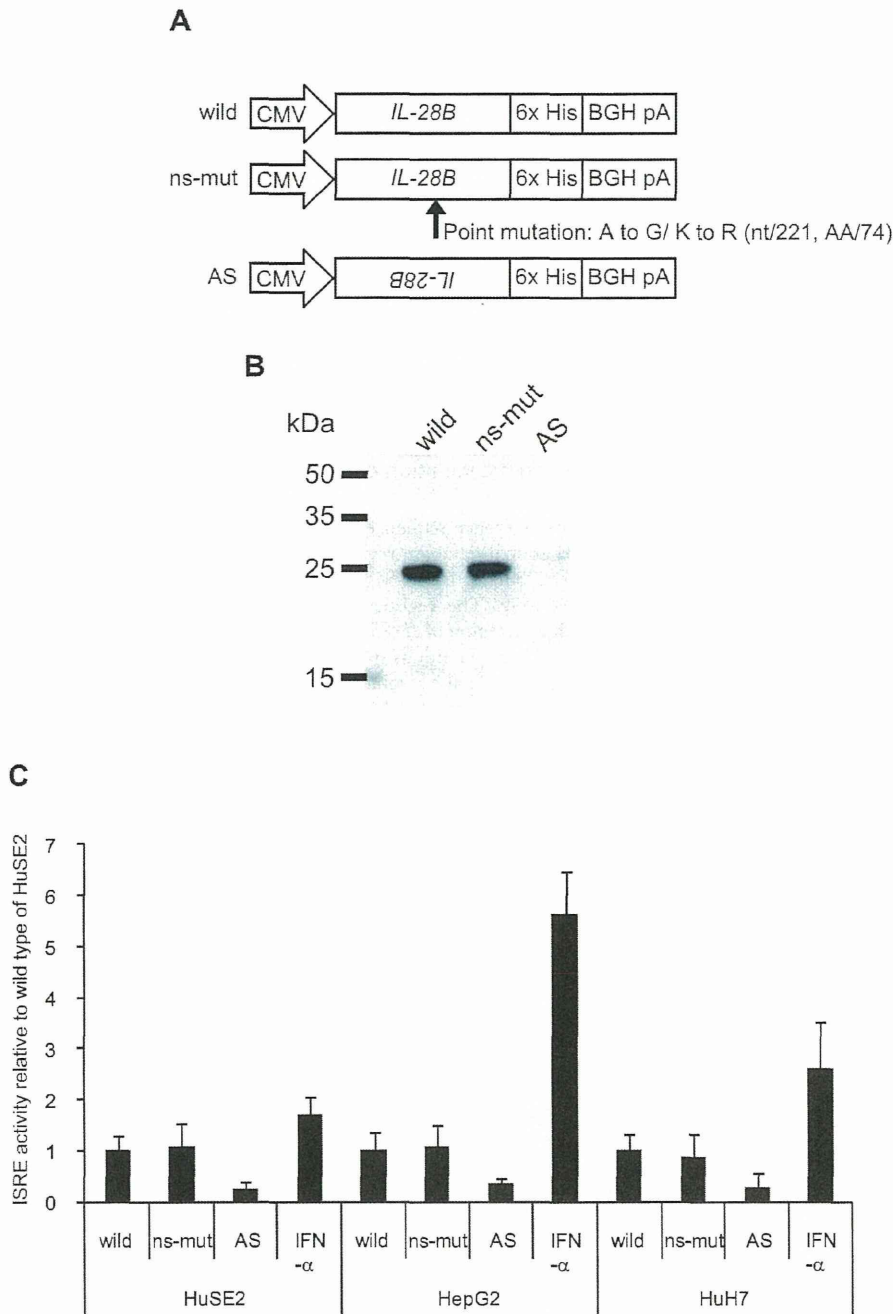


**Figure 5. The purification and the activity of recombinant IL-28B with or without nsSNP.** (A) The 6×His-tagged expression plasmid of wild type, ns-mut, or AS controlled by the CMV promoter was transfected into 293F cells. Schematics are the wild type, ns-mut and AS used in the transfection experiments. The procedure for recombinant protein purification is described in the materials and methods section. (B) The purified products were confirmed by immunoblotting using anti-IL28B antibody and the secondary antibody. The prepared proteins were loaded onto a 12% polyacrylamide gel. Bands corresponding to the expected molecular weight of IL-28B were observed in the wild type and ns-mut lanes. (C) For luciferase assay, HeLa cells were seeded into a 96-well plate at $10^4$ cells/well and transfected with pISRE-Luc and pGL4.74 control vector before 16 h of IFN-α or IL-28B stimulation. Five ng/mL of IL-28B wild or ns-mut was added to the culture medium. Flow-though liquid from AS expression was used as a negative control. IFN-α (100 U/mL) was added for positive control of ISRE activity. The luciferase activities were normalized with Renilla activities and data are presented as fold induction from the basal promoter activation of the wild type. Bars indicate the means ± SD of triplicate determinations and the results are from one of three experiments.
doi:10.1371/journal.pone.0026620.g005

**Table 2.** The variations of TA repeat in *IL-28A* and *28B*.

| Gene | Data | Location | |
| | | rs72284792*[1] | rs72258881 |
| --- | --- | --- | --- |
| *IL-28A* | RefSeq. (hg19) | $(TA)_8$ | |
| | Cloning | $(TA)_8$ | |
| *IL-28B* | RefSeq. (hg19) | | $(TA)_{13}$ |
| | Cloning | | $(TA)_{10-18}$ |

*[1]The ID represents rs72258881, rs59702201, and rs67461793 because these three are located in the same genomic region, the TA repeat.
doi:10.1371/journal.pone.0026620.t002

expression (Fig. 6A). These cells were treated with 100 U/mL of IFN-α and 3 μg/mL of LPS. The results indicated that the variation in the $(TA)_n$ number at this polymorphic locus differentially regulates transcription. The transcriptional activation of the luciferase reporter gene was increased according to the $(TA)_n$ number (Fig. 6B).

## Discussion

Four independent GWAS approaches have revealed the significant SNPs associated with response to PEG-IFNα/RBV therapy for CHC [12,13,14,19]. These significant SNPs were found around *IL-28B* but not *IL-28A*. The SNPs found in clinical studies to determine the outcome of HCV therapy were rs12979860 and rs8099917, because they showed the statistical significance in each study [12,13,14,19]. However, several SNPs around *IL-28B* were in strong LD ($r^2>0.96$) in JPT and CEU populations, although relatively low LD was predicted in the YRI population [16], and so it might be difficult to determine the most informative SNP [16]. These results suggest that any of the SNPs contained in this region could be of predictive value.

As reported in previous studies, transcription of *IL-28A/B* was upregulated in the TT genotype of rs8099917, which was associated with SVR [13,14,20], suggesting that the expression levels of *IL-28B* could be one of the key factors to clear HCV under PEG-IFNα/RBV therapy and could also affect spontaneous clearance of acute HCV infection [15]. To elucidate this question, we examined the function of the SNPs around the *IL-28B* gene to identify those SNPs affecting *IL-28B* expression. The new findings are as follows: 1) the gene structure of *IL-28B* comprised six exons in the several cell lines tested, although it was registered as having five exons in the CCDS database of NCBI. 2) The substitution of intron SNPs and non-synonymous SNPs in the *IL-28B* gene did not influence the expression levels or function. 3) Increased numbers of TA repeats in the promoter region of the *IL-28B* gene enhanced the transcription activity and expression level of the *IL-28B* gene. Because administration of IL-28B has been shown to have antiviral effects [21,22,23], lower expression of IL-28B might lead to a decrease in this effect.
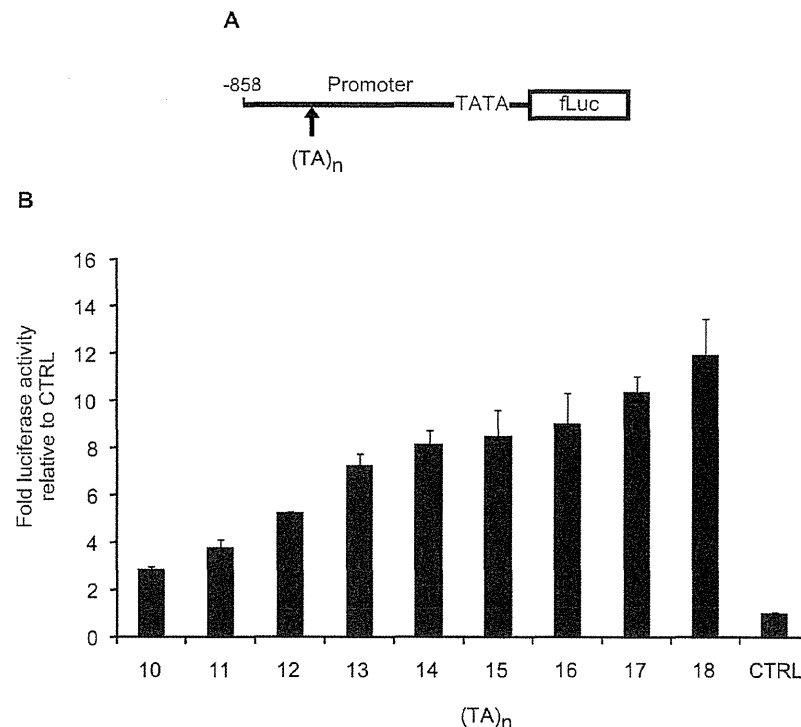


**Figure 6. Luciferase assay of $(TA)_n$ number.** (A) *IL-28B* promoter subfragment (nt −858 to +30) modifying $(TA)_n$ number from 10 to 18 was constructed in the pGL4 vector. (B) Raji cells were co-transfected with pGL4 plasmids (0.05 g), and pGL4.74 control plasmid (0.05 g), and tested for firefly as well as renilla luciferase after LPS stimulation (3 μg/mL) for 4 h following IFN-α treatment (100 U/mL) for 16 h. These cells were seeded into a 96-well plate at $10^4$ cells/well. The luc activities were normalized with renilla activities and data are presented as fold induction from the activation of the control vector. Bars, the means ± SD of triplicate determinations and the results are from one of three experiments. Statistical analyses are shown in table S4 to avoid complication.
doi:10.1371/journal.pone.0026620.g006

- 1358 -

The locations of two SNPs associated with response to HCV therapy, rs8099917 and rs12979860, are approximately 8 kb and 3 kb upstream of *IL-28B* gene, respectively. Because these SNPs, which showed the greatest statistical significance in the previous study, are located far from the *IL-28B* gene, another approach was required to determine the effect of the SNPs. In this study, broad $(TA)_n$ variations were observed in rs8099917 heterozygotes among CHC patients. Interestingly, a combination of TG and 11/12 genotype was strongly associated with NVR, whereas patients harboring the 12/13 genotype showed a virological response, regardless of the TG genotype (rs8099917). In clinical practice, genetic diagnosis using TA variation, following the primary classification of rs8099917 genotype, could improve the prediction of treatment response for CHC patients with the rs8099917 TG genotype. It is not clear whether the variation originates from genetic or epigenetic mechanisms. In addition, as the frequency of TA variation might be dependent on the particular population, further study will be needed to compare the frequency in several populations. A long TA repeat, over $(TA)_{13}$, was observed in healthy volunteers and showed potential for higher gene expression compared with under $(TA)_{13}$ constructs *in vitro*. It may be possible that spontaneous clearance of HCV infection and CHC patients are affected by this region because this also is dependent on *IL-28B* genotype [15,19]. In our speculation, the combination of both TA variation and the landmark SNPs, rs8099917 and rs12979860, might improve the prediction value. In addition, convenient diagnosis method to detect the TA variation like SNPs typing is needed since the present capillary techniques are relative complexity compared with SNPs typing.

In the international database, some SNPs ID are registered in the TA repeat region, located in the regulatory regions of the *IL-28A* and *IL-28B* gene, rs72284792 and rs7225881, respectively, whereas in our analysis separating *IL-28A* from *IL-28*, TA variation was detected only in the *IL-28B* region. SNP data often have been collected using next generation sequencing and based on short sequence reads. Unfortunately, the sequence similarity between *IL-28A* and *IL-28B* is over 90% from the CpG island to the region downstream of 3'-UTR. Alignment failure would occur for a high percentage of sequences when analyzed with software using general algorithms.

Effects of insertion/deletion (indel) polymorphism are known in the field of pharmacogenetic research. A polymorphism in the promoter of the uridine diphosphoglucuronosyl transferase 1A1 (*UGT 1A1*) gene has been shown to cause Crigler-Najjar syndrome types I and II and Gilbert syndrome, a benign form of unconjugated hyperbilirubinemia, and the occurrence of severe toxic events in irinotecan (known as CPT-11) administration [24,25,26]. The polymorphism consists of a $(TA)_n$ repeat in the 5'-promoter region [24,26,27], similar to that in this study. The range of repeat numbers is from $(TA)_5$ to $(TA)_8$ in the *UGT 1A1* gene [28]. The genetic disorder of the TA repeat length affects enzyme activity. The hepatic bilirubin *UGT 1A1* activity of individuals with Gilbert's syndrome is <30% of normal [29]. Irinotecan is used or under evaluation for a broad spectrum of solid tumors. Irinotecan pharmacokinetic parameters display a wide inter-patient variability and are involved in the genesis of toxic side effects [30,31,32,33]. Based on the polymorphism of the TA repeat, previous papers reported the association of irinotecan-induced severe toxicity with Gilbert's syndrome [34,35,36]. The value of genetic diagnosis of the *UGT1A1* polymorphisms prior to irinotecan chemotherapy has been corroborated in a previous study [37]. As similar characteristics were observed in the upstream region of *IL-28B*, the $(TA)_n$ repeat might be associated with disease progression as well as response to anti-HCV treatment.

In terms of epigenetic aspects, the TA variation of *IL-28B* was also suspected to be related to microsatellite instability, because a gap between the significant SNPs and TA variation was observed in this study. DNA mismatch repair (MMR) deficiency causes a high frequency of microsatellite instability (MSI-H), which is characterized by length alterations within simple repeated sequences, microsatellites. Lynch syndrome is primarily due to germline mutations in one of the DNA MMR genes, hMLH1 or hMSH2 [38]. MSI-H is also observed in <15% of colorectal, gastric and endometrial cancers, where it is associated with the hypermethylation of the promoter region of hMLH1 [39,40]. The diagnosis of MSI-H in cancers is therefore useful for identifying patients with Lynch syndrome and the efficacy of chemotherapy [41,42,43,44,45,46].

In conclusion, a (TA) dinucleotide repeat, rs72258881, located in the promoter region, was discovered by our functional studies of the proximal SNPs around *IL-28B*; the transcriptional activity of the promoter increased gradually in a $(TA)_n$ length-dependent manner. Combination diagnosis based on rs8099917 and rs72258881 might provide improved prediction because the $(TA)_n$ variation of *IL-28B* was observed but not that of *IL-28A*. The further study is needed to reveal the association with treatment response using clinical specimens of CHC. These findings suggest that the dinucleotide repeat could be associated with the transcriptional activity of *IL-28B* as well as constituting a predictor to improve prediction of the response to interferon-based HCV treatment.

## Supporting Information

**Figure S1 Sequence alignment of *IL-28A/B* cDNA retrieved from the database.** The cDNA sequences of *IL-28A/B* were retrieved from the international database using accession number. The cDNA data reported by Sheppard et al. are AY129148 (*IL-28A*) and AY129149 (*IL-28B*) indicated with '_S' in the figure, and that of Kotenko et al. are AY184373 (*IL-28A*) and AY184374 (*IL-28B*) indicated with '_K'. Dashed boxes show the start codon predicted by computational analysis of the human genome reported by Sheppard et al. and Kotenko et al. The sequence alignment was calculated with Lasergene software (DNASTAR, Madison, WI).
(PDF)

**Figure S2 Structural similarity between *IL-28A* and *IL-28B*.** (A) Schematic of *IL-28A/B* gene location (UCSC genome browser). Boxes show the region representing high levels of structural similarity around *IL-28A/B*. (B) Modified schematic of structural similarity with a percentage. (C) Alignment between IL-28A and IL-28B from the CpG island to the region downstream of 3'-UTR. Homologous regions are shown by red characters. High levels of structural similarity were observed in CpG island, regulatory and gene region bypassing the in/del site.
(PDF)

**Figure S3 Innate immune receptor expression related to IL-28B regulation.** The relevant receptors for this study were confirmed by PCR using specific primers. (A) The mRNA expression of TLR4 was detected in cell lines, HeLa, Jurkat, MT-2, Raji, and PBMC. (B) For the study of cytokine-receptor association, the expression of IL-28RA and IL-10RB second receptor were examined using cDNA obtained from HuH7, HepG2, and HuSE2 cells. Samples without reverse transcriptase were prepared as a negative control in addition to the checking of genome contamination.
(PDF)

**Figure S4 Direct sequencing analysis of TA repeat.** In the first step to determine $(TA)_n$ genotypes, direct sequencing was

applied to amplicons of *IL-28A* or *28B* separated by gel electrophoresis. Homozygotes of TA repeat showed clear patterns and a high quality value in the bar above, whereas the patterns of heterozygotes were mixed because the length differed between alleles. The mixed patterns are shown in dashed boxes. These mixed products were cloned into the pGEM-Teasy vector to isolate and count the $(TA)_n$ number by sequencing of both alleles. (PDF)

**Table S1**
(DOC)

**Table S2**
(DOC)

**Table S3**
(DOC)

**Table S4**
(DOC)

## Author Contributions

Conceived and designed the experiments: MS YT MN TW MM. Performed the experiments: MS YT. Analyzed the data: MS YT. Contributed reagents/materials/analysis tools: MS YT MN TW MM. Wrote the paper: MS YT MN TW MM.

## References

1. Kotenko SV, Gallagher G, Baurin VV, Lewis-Antes A, Shen M, et al. (2003) IFN-lambdas mediate antiviral protection through a distinct class II cytokine receptor complex. Nat Immunol 4: 69–77.
2. Sheppard P, Kindsvogel W, Xu W, Henderson K, Schlutsmeyer S, et al. (2003) IL-28, IL-29 and their class II cytokine receptor IL-28R. Nat Immunol 4: 63–68.
3. Mordstein M, Kochs G, Dumoutier L, Renauld JC, Paludan SR, et al. (2008) Interferon-lambda contributes to innate immunity of mice against influenza A virus but not against hepatotropic viruses. PLoS Pathog 4: e1000151.
4. Sommereyns C, Paul S, Staeheli P, Michiels T (2008) IFN-lambda (IFN-lambda) is expressed in a tissue-dependent fashion and primarily acts on epithelial cells in vivo. PLoS Pathog 4: e1000017.
5. Doyle SE, Schreckhise H, Khuu-Duong K, Henderson K, Rosler R, et al. (2006) Interleukin-29 uses a type 1 interferon-like program to promote antiviral responses in human hepatocytes. Hepatology 44: 896–906.
6. Marcello T, Grakoui A, Barba-Spaeth G, Machlin ES, Kotenko SV, et al. (2006) Interferons alpha and lambda inhibit hepatitis C virus replication with distinct signal transduction and gene regulation kinetics. Gastroenterology 131: 1887–1898.
7. Zhou Z, Hamming OJ, Ank N, Paludan SR, Nielsen AL, et al. (2007) Type III interferon (IFN) induces a type I IFN-like response in a restricted subset of cells through signaling pathways involving both the Jak-STAT pathway and the mitogen-activated protein kinases. J Virol 81: 7749–7758.
8. Bartlett NW, Buttigieg K, Kotenko SV, Smith GL (2005) Murine interferon lambdas (type III interferons) exhibit potent antiviral activity in vivo in a poxvirus infection model. J Gen Virol 86: 1589–1596.
9. Brand S, Zitzmann K, Dambacher J, Beigel F, Olszak T, et al. (2005) SOCS-1 inhibits expression of the antiviral proteins 2′,5′-OAS and MxA induced by the novel interferon-lambdas IL-28A and IL-29. Biochem Biophys Res Commun 331: 543–548.
10. Robek MD, Boyd BS, Chisari FV (2005) Lambda interferon inhibits hepatitis B and C virus replication. J Virol 79: 3851–3854.
11. Zhu H, Butera M, Nelson DR, Liu C (2005) Novel type I interferon IL-28A suppresses hepatitis C viral RNA replication. Virol J 2: 80.
12. Ge D, Fellay J, Thompson AJ, Simon JS, Shianna KV, et al. (2009) Genetic variation in IL28B predicts hepatitis C treatment-induced viral clearance. Nature 461: 399–401.
13. Suppiah V, Moldovan M, Ahlenstiel G, Berg T, Weltman M, et al. (2009) IL28B is associated with response to chronic hepatitis C interferon-alpha and ribavirin therapy. Nat Genet 41: 1100–1104.
14. Tanaka Y, Nishida N, Sugiyama M, Kurosaki M, Matsuura K, et al. (2009) Genome-wide association of IL28B with response to pegylated interferon-alpha and ribavirin therapy for chronic hepatitis C. Nat Genet 41: 1105–1109.
15. Thomas DL, Thio CL, Martin MP, Qi Y, Ge D, et al. (2009) Genetic variation in IL28B and spontaneous clearance of hepatitis C virus. Nature 461: 798–801.
16. Tanaka Y, Nishida N, Sugiyama M, Tokunaga K, Mizokami M (2010) lambda-Interferons and the single nucleotide polymorphisms: A milestone to tailor-made therapy for chronic hepatitis C. Hepatol Res 40: 449–460.
17. Siren J, Pirhonen J, Julkunen I, Matikainen S (2005) IFN-alpha regulates TLR-dependent gene expression of IFN-alpha, IFN-beta, IL-28, and IL-29. J Immunol 174: 1932–1937.
18. Livak KJ, Schmittgen TD (2001) Analysis of relative gene expression data using real-time quantitative PCR and the 2(-Delta Delta C(T)) Method. Methods 25: 402–408.
19. Rauch A, Kutalik Z, Descombes P, Cai T, Di Iulio J, et al. (2010) Genetic variation in IL28B is associated with chronic hepatitis C and treatment failure: a genome-wide association study. Gastroenterology. pp 138-1338–1345, 1345 e1331–1337.
20. Fukuhara T, Taketomi A, Motomura T, Okano S, Ninomiya A, et al. (2010) Variants in IL28B in liver recipients and donors correlate with response to peg-

interferon and ribavirin therapy for recurrent hepatitis C. Gastroenterology. pp 139-1577–1585, 1585 e1571–1573.
21. Ank N, Iversen MB, Bartholdy C, Staeheli P, Hartmann R, et al. (2008) An important role for type III interferon (IFN-lambda/IL-28) in TLR-induced antiviral activity. J Immunol 180: 2474–2485.
22. Ank N, West H, Bartholdy C, Eriksson K, Thomsen AR, et al. (2006) Lambda interferon (IFN-lambda), a type III IFN, is induced by viruses and IFNs and displays potent antiviral activity against select virus infections in vivo. J Virol 80: 4501–4509.
23. Contoli M, Message SD, Laza-Stanca V, Edwards MR, Wark PA, et al. (2006) Role of deficient type III interferon-lambda production in asthma exacerbations. Nat Med 12: 1023–1026.
24. Bosma PJ, Chowdhury JR, Bakker C, Gantla S, de Boer A, et al. (1995) The genetic basis of the reduced expression of bilirubin UDP-glucuronosyltransferase 1 in Gilbert's syndrome. N Engl J Med 333: 1171–1175.
25. Monaghan G, Ryan M, Seddon R, Hume R, Burchell B (1996) Genetic variation in bilirubin UPD-glucuronosyltransferase gene promoter and Gilbert's syndrome. Lancet 347: 578–581.
26. Raijmakers MT, Jansen PL, Steegers EA, Peters WH (2000) Association of human liver bilirubin UDP-glucuronyltransferase activity with a polymorphism in the promoter region of the UGT1A1 gene. J Hepatol 33: 348–351.
27. Sato H, Adachi Y, Koiwai O (1996) The genetic basis of Gilbert's syndrome. Lancet 347: 557–558.
28. Beutler E, Gelbart T, Demina A (1998) Racial variability in the UDP-glucuronosyltransferase 1 (UGT1A1) promoter: a balanced polymorphism for regulation of bilirubin metabolism? Proc Natl Acad Sci U S A 95: 8170–8174.
29. Yamamoto K, Sato H, Fujiyama Y, Doida Y, Bamba T (1998) Contribution of two missense mutations (G71R and Y486D) of the bilirubin UDP glycosyltransferase (UGT1A1) gene to phenotypes of Gilbert's syndrome and Crigler-Najjar syndrome type II. Biochim Biophys Acta 1406: 267–273.
30. Gupta E, Lestingi TM, Mick R, Ramirez J, Vokes EE, et al. (1994) Metabolic fate of irinotecan in humans: correlation of glucuronidation with diarrhea. Cancer Res 54: 3723–3725.
31. Gupta E, Mick R, Ramirez J, Wang X, Lestingi TM, et al. (1997) Pharmacokinetic and pharmacodynamic evaluation of the topoisomerase inhibitor irinotecan in cancer patients. J Clin Oncol 15: 1502–1510.
32. Rowinsky EK, Grochow LB, Ettinger DS, Sartorius SE, Lubejko BG, et al. (1994) Phase I and pharmacological study of the novel topoisomerase I inhibitor 7-ethyl-10-[4-(1-piperidino)-1-piperidino]carbonyloxycamptothecin (CPT-11) administered as a ninety-minute infusion every 3 weeks. Cancer Res 54: 427–436.
33. Iyer L, King CD, Whitington PF, Green MD, Roy SK, et al. (1998) Genetic predisposition to the metabolism of irinotecan (CPT-11). Role of uridine diphosphate glucuronosyltransferase isoform 1A1 in the glucuronidation of its active metabolite (SN-38) in human liver microsomes. J Clin Invest 101: 847–854.
34. Sugatani J, Yamakawa K, Yoshinari K, Machida T, Takagi H, et al. (2002) Identification of a defect in the UGT1A1 gene promoter and its association with hyperbilirubinemia. Biochem Biophys Res Commun 292: 492–497.
35. Iyanagi T, Emi Y, Ikushiro S (1998) Biochemical and molecular aspects of genetic disorders of bilirubin metabolism. Biochim Biophys Acta 1407: 173–184.
36. Wasserman E, Myara A, Lokiec F, Goldwasser F, Trivin F, et al. (1997) Severe CPT-11 toxicity in patients with Gilbert's syndrome: two case reports. Ann Oncol 8: 1049–1051.
37. Sadee W, Dai Z (2005) Pharmacogenetics/genomics and personalized medicine. Hum Mol Genet 14 Spec No. 2: R207-214.
38. Modrich P (1994) Mismatch repair, genetic stability, and cancer. Science 266: 1959–1960.
39. Lengauer C, Kinzler KW, Vogelstein B (1997) DNA methylation and genetic instability in colorectal cancer cells. Proc Natl Acad Sci U S A 94: 2545–2550.

40. Lengauer C, Kinzler KW, Vogelstein B (1997) Genetic instability in colorectal cancers. Nature 386: 623–627.

41. Kim GP, Colangelo LH, Paik S, O'Connell MJ, Kirsch IR, et al. (2007) Predictive value of microsatellite instability-high remains controversial. J Clin Oncol 25: 4857; author reply 4857–4858.

42. Elsaleh H, Joseph D, Grieu F, Zeps N, Spry N, et al. (2000) Association of tumour site and sex with survival benefit from adjuvant chemotherapy in colorectal cancer. Lancet 355: 1745–1750.

43. Gryfe R, Kim H, Hsieh ET, Aronson MD, Holowaty EJ, et al. (2000) Tumor microsatellite instability and clinical outcome in young patients with colorectal cancer. N Engl J Med 342: 69–77.

44. Ribic CM, Sargent DJ, Moore MJ, Thibodeau SN, French AJ, et al. (2003) Tumor microsatellite-instability status as a predictor of benefit from fluorouracil-based adjuvant chemotherapy for colon cancer. N Engl J Med 349: 247–257.

45. Popat S, Hubner R, Houlston RS (2005) Systematic review of microsatellite instability and colorectal cancer prognosis. J Clin Oncol 23: 609–618.

46. Sinicrope FA, Rego RL, Halling KC, Foster N, Sargent DJ, et al. (2006) Prognostic impact of microsatellite instability and DNA ploidy in human colon carcinoma patients. Gastroenterology 131: 729–737.

# Hepatitis C Virus Reveals a Novel Early Control in Acute Immune Response

Noëlla Arnaud[1], Stéphanie Dabo[1], Daisuke Akazawa[2], Masayoshi Fukasawa[3], Fumiko Shinkai-Ouchi[3], Jacques Hugon[4], Takaji Wakita[2], Eliane F. Meurs[1]*

1 Institut Pasteur, Hepacivirus and Innate Immunity, Paris, France, 2 National Institute of Infectious Diseases, Department of Virology II, Tokyo, Japan, 3 National Institute of Infectious Diseases, Department of Biochemistry and Cell Biology, Tokyo, Japan, 4 Institut du Fer à Moulin, INSERM UMRS 839, Paris, France

## Abstract

Recognition of viral RNA structures by the intracytosolic RNA helicase RIG-I triggers induction of innate immunity. Efficient induction requires RIG-I ubiquitination by the E3 ligase TRIM25, its interaction with the mitochondria-bound MAVS protein, recruitment of TRAF3, IRF3- and NF-κB-kinases and transcription of Interferon (IFN). In addition, IRF3 alone induces some of the Interferon-Stimulated Genes (ISGs), referred to as early ISGs. Infection of hepatocytes with Hepatitis C virus (HCV) results in poor production of IFN despite recognition of the viral RNA by RIG-I but can lead to induction of early ISGs. HCV was shown to inhibit IFN production by cleaving MAVS through its NS3/4A protease and by controlling cellular translation through activation of PKR, an eIF2α-kinase containing dsRNA-binding domains (DRBD). Here, we have identified a third mode of control of IFN induction by HCV. Using HCVcc and the Huh7.25.CD81 cells, we found that HCV controls RIG-I ubiquitination through the di-ubiquitine-like protein ISG15, one of the early ISGs. A transcriptome analysis performed on Huh7.25.CD81 cells silenced or not for PKR and infected with JFH1 revealed that HCV infection leads to induction of 49 PKR-dependent genes, including ISG15 and several early ISGs. Silencing experiments revealed that this novel PKR-dependent pathway involves MAVS, TRAF3 and IRF3 but not RIG-I, and that it does not induce IFN. Use of PKR inhibitors showed that this pathway requires the DRBD but not the kinase activity of PKR. We then demonstrated that PKR interacts with HCV RNA and MAVS prior to RIG-I. In conclusion, HCV recruits PKR early in infection as a sensor to trigger induction of several IRF3-dependent genes. Among those, ISG15 acts to negatively control the RIG-I/MAVS pathway, at the level of RIG-I ubiquitination. These data give novel insights in the machinery involved in the early events of innate immune response.

## Introduction

IFN induction in response to several RNA viruses involves the intracytosolic pathogen recognition receptor (PRR) CARD-containing DexD/H RNA helicase RIG-I. Following its binding to viral RNA, RIG-I undergoes a change in its conformation through Lys63-type ubiquitination by the E3 ligase TRIM25. This allows its N-terminal CARD domain to interact with the CARD domain of the mitochondria-bound adapter MAVS [1,2]. MAVS then interacts with TRAF3 to further recruit downstream IRF3 and NF-κB-activating kinases, that stimulate the IFNβ promoter in a cooperative manner. In addition, IRF3 stimulates directly the promoters of some interferon-induced genes (early ISGs) while NF-κB stimulates that of inflammatory cytokines [3].

The RNA of Hepatitis C virus (HCV) has an intrinsic ability to trigger IFNβ induction through RIG-I [4,5,6]. Yet HCV is a poor IFN inducer. One reason for this comes from the ability of its NS3 protease to cleave MAVS [7]. Another relates to the ability of HCV to trigger activation of the dsRNA-dependent eIF2α kinase PKR [8,9] which leads to inhibition of IFN expression through general control of translation while the viral genome can be translated from its eIF2α-insensitive IRES structure [8].

HCV infection can trigger important intrahepatic synthesis of several IFN-induced genes (ISGs) in patients [10,11] and in animal models of infection in chimpanzees [12]. Expression of ISGs can be explained at least in part by the ability of HCV to activate the IFN-producing pDCs in the liver through cell-to-cell contact with HCV-infected cells [13]. Intriguingly, despite the recognized antiviral activity of a number of these ISGs, their high expression paradoxically represents a negative predictive marker for the response of these patients to standard combination IFN/ribavirin therapy [14,15,16]. The ubiquitine-like protein ISG15 is among the ISGs which are the most highly induced by HCV [16] and was recently shown to act as a pro-HCV agent [17]. Interestingly, ISG15 was also shown to control RIG-I activity through ISGylation [18].

Here, we show that HCV controls IFN induction at the level of RIG-I ubiquitination through the ubiquitine-like protein ISG15, one of the early ISGs. Use of small interfering RNA (siRNA) targeting to compare the effect of ISG15 to that of PKR on IFN induction and HCV replication led to the unexpected finding that HCV infection triggers induction of ISG15 and other ISGs by using PKR as an adapter through its N terminal dsRNA binding domain. This recruits a signaling pathway which involves MAVS, TRAF3

– 1362 –

## Author Summary

Hepatitis C Virus (HCV) is a poor interferon (IFN) inducer, despite recognition of its RNA by the cytosolic RNA helicase RIG-I. This is due in part through cleavage of MAVS, a downstream adapter of RIG-I, by the HCV NS3/4A protease and through activation of the eIF2α-kinase PKR to control IFN translation. Here, we show that HCV also inhibits RIG-I activation through the ubiquitin-like protein ISG15 and that HCV triggers rapid induction of 49 genes, including ISG15, through a novel signaling pathway that precedes RIG-I and involves PKR as an adapter to recruit MAVS. Hence, we propose to divide the acute response to HCV infection into one early (PKR) and one late (RIG-I) phase, with the former controlling the latter. Furthermore, these data emphasize the need to check compounds designed as immune adjuvants for activation of the early acute phase before using them to sustain innate immunity.

and IRF3 but not RIG-I. Altogether, our results present a novel mechanism by which HCV uses PKR and ISG15 to attenuate the innate immune response.

## Results

### HCV infection negatively controls RIG-I ubiquitination

We recently reported that the HCV permissive Huh7.25.CD81 cells [19] that we used to identify the pro-HCV action of PKR, did not induce IFN in response to HCV infection, unless after ectopic expression of TRIM25 [8]. We started this study by investigating at which level this defect could occur. A $P_{358}L$ substitution in the endogenous TRIM25 of these cells, revealed by sequence analysis, proved to have no incidence of the ability of TRIM25 to participate in the IFN induction process. Indeed, ectopic expression of a TRIM25 $P_{358}L$ construct was as efficient as a TRIM25wt construct to increase IFN induction in the Huh7.25.CD81 cells, after infection with Sendai virus (SeV) (**Figure 1A**). Like some other members of the TRIM family, TRIM25 is localized in both the cytosol and nucleus and is induced upon IFN treatment [20]. No specific difference between the cellular localization of TRIM25 was observed in the Huh7.25.CD81 cells when compared to Huh7 cells or Huh7.5 cells, which rules out a role for a cellular mislocalization in its inability to participate in IFN induction (**Figure 1B**). TRIM25 was also efficiently induced by IFN (**Figure 1B and Figure S1**). We assayed whether increasing TRIM25 upon IFN treatment could mimic the effect of its ectopic expression and restore IFN induction in response to HCV infection. However, this resulted only in a poor stimulation of an IFNβ promoter (3 to 5-fold), in contrast to its effect upon SeV infection (230-fold) (**Figure 1C**). Similarly, HCV infection at higher m.o.i, as an attempt to favour recognition of RIG-I by the viral RNA, only modestly increased IFN induction (**Figure 1D**). TRIM25 plays an essential role in IFN induction through RIG-I ubiquitination [1]. We then analysed whether this step was affected by HCV infection in the Huh7.25.CD81 cells. The results showed that, in contrast to SeV infection used as control, HCV infection could not trigger RIG-I ubiquitination, unless the cells are supplied with ectopic TRIM25 (**Figure 1E**). Thus, HCV infection appears to mediate a control on IFN induction through regulation of RIG-I ubiquitination.
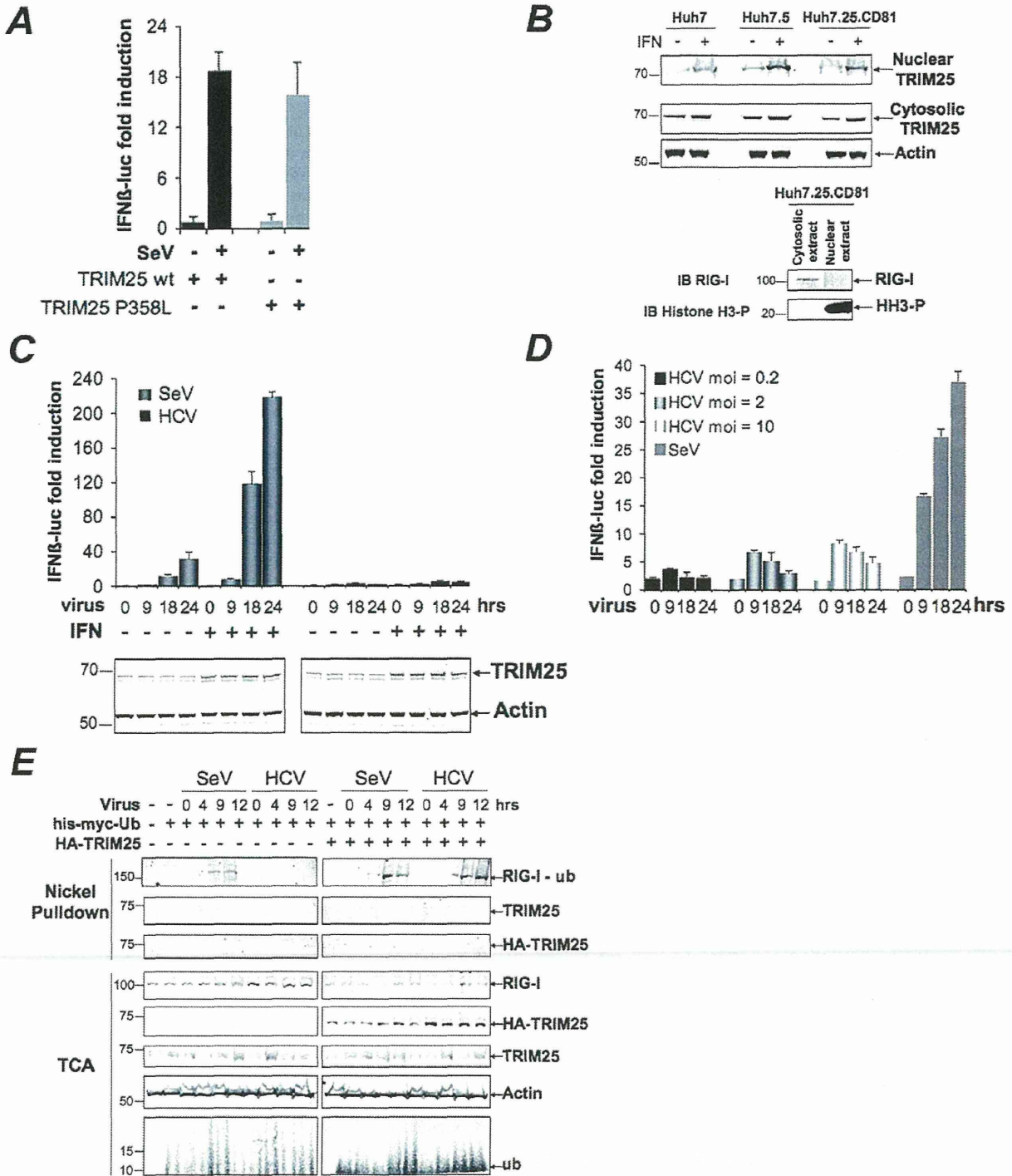
### HCV controls RIG-I ubiquitination through ISG15

Inhibition of the function of TRIM25 or RIG-I ubiquitination has been suggested to occur via the small ubiquitin-like protein

ISG15 and the process of ISGylation [18,21]. We then analysed whether ISG15 was involved in the control of RIG-I ubiquitination upon HCV infection. For this, we chose a transient transfection approach using siRNAs targeting ISG15 in the Huh7.25.CD81 cells. Indeed, this resulted in a strong ubiquitination of RIG-I at 9 hrs and 12 hrs post-HCV infection, which was equivalent to that observed in cells supplied with ectopic TRIM25 (**Figure 2A**). A similar result was obtained after JFH1 infection in the Huh7 cells, used as another HCV-permissive cell line (**Figure S2**). Thus, ISG15 can control RIG-I ubiquitination in different cells infected by HCV. We next investigated whether ISGylation was involved in this process. Absence of detection of RIG-I ubiquitination after HCV infection of the Huh7.25.CD81 cells precludes direct analysis of the effect of ISG15 on RIG-I. We used an IFNβ-luc reporter assay instead, as it proved to be sensitive enough to detect some IFN induction in response to JFH1 infection in those cells (see Figure 1D). We found that IFN induction increased when cells were transfected with siRNAs targeting ISG15 while it decreased in cells overexpressing IGS15 (**Figure 2B**). Expression of ISG15 in the presence of the E1, E2 and E3 ligases involved in ISGylation (respectively Ube1L, UbcH8 and HERC5) [22] further inhibits IFNβ induction (**Figure 2B**). Similar results were observed upon infection with Sendai virus (**Figure S3**). The ISGylation process is strictly dependent on the presence of the E1 ligase Ube1L [23]. Indeed, enhanced IFN promoter activity has been observed in Ube1L−/− cells in response to NDV [18]. In accord with this, depletion of endogenous Ube1L from the Huh7.25.CD81 cells (**Figure S4**), as such or after ectopic expression of ISG15, UbcH8 and HERC5, resulted in an increase in IFNβ induction after infection with HCV (**Figure 2B**). We then analysed the effect of siISG15 on IFNβ induction after infecting the cells with HCV up to 72 hours, in order to pass through the 24 hr time-point where the signaling pathway leading to the transcription of this gene is expected to stop because of the NS3/4A-mediated cleavage of MAVS [8]. The results show that, whereas IFNβ transcription was indeed strongly inhibited after 24 hr in the control cells, it still occurred significantly in the cells expressing siRNA ISG15 (**Figure 2C**). Previous data have shown a positive role for ISG15 on HCV production [24,25]. In accord with this, silencing of ISG15 resulted in clear inhibition of HCV RNA expression with however no significant consequence on the ability of the virions produced to re-infect fresh cells (**Figure 2D**). Analysis of expression of MAVS and NS3, as well as the expression of the core protein as another example of viral protein, then showed that the depletion of ISG15 both decreased and delayed the expression of the viral proteins as compared to the siRNA control cells and that this was correlated by a delay in the NS3/4A-mediated cleavage of MAVS (**Figure 2E**). These results show that ISG15 controls the process of IFN induction during HCV infection by interfering with RIG-I ubiquitination through an ISGylation process and by boosting efficient accumulation of NS3, among other viral proteins, thus favouring its negative control on IFN induction by cleavage of MAVS.

### ISG15 strengthens the pro-HCV activity of PKR

ISG15 ([24,25] and this study) and PKR [8,9] emerge as two ISGs with pro-HCV activities, instead of playing an antiviral role. We then assayed the effect of a combined depletion of PKR and ISG15 on HCV replication and IFN expression in the Huh7.25.CD81 cells. As shown in Figure 2 D and B, siRNAs targeting ISG15 were sufficient both to inhibit HCV replication (**Figure 3A**) and to increase IFNβ expression, either measured by RTqPCR (**Figure 3B**) or by using an IFNβ-luciferase reporter

**Figure 1. HCV infection negatively controls RIG-I ubiquitination.** (A) Huh7.25.CD81 cells were transfected for 24 hrs with 150 ng of the pGL2-IFNβ-FLUC; 40 ng of the pRL-TK-RLUC reporter plasmids alone or in presence of 150 ng of a plasmid expressing HA-TRIM25, either as such (TRIM25wt) or containing the $P_{358}L$ substitution (a SNP rs75467764 with no reported pathology). Cells were infected or not with SeV (40 HAU/ml) for 24 hrs. IFN expression was expressed as fold induction of luciferase activity. Error bars represent the mean ± S.D. for triplicates. (B) Huh7, Huh7.5 and Huh7.25.CD81 cells were either untreated or treated with 500 U/ml IFNα for 24 hrs. TRIM25 was detected by immunoblot after preparation of nuclear and cytosolic fractions from 25 μg of cell extracts. Detection of Actin, RIG-I and phosphorylated Histone 3 (HH3-P) served as controls. (C–D) Huh7.25.CD81 cells were transfected with the reporter plasmids as in A, a few hours before being treated with 500 U/ml IFNα for 24 hrs (C) or left untreated (C or D). They were then infected with Sendai virus (40 HAU/ml) or with JFH1 at an m.o.i of 0.2 (C) or increasing from 0.2 to 10 (D). At the times indicated, IFN expression was expressed as fold induction of luciferase activity. Error bars represent the mean ± S.D. for triplicates. Induction of

assay (**Figure 3C**). Very limited additional effect was observed in the concomitant presence of siRNAs targeting PKR. (**Figure 3B**). Interestingly, we noticed that expression of luciferase from the IFNβ promoter increased throughout the first 18 hours of HCV infection in the siISG15 cells (**Figure 3C**). This was intriguing as it should have been inhibited after 12 hours of HCV infection through the eIF2α kinase activity of PKR and its control on translation [8]. We therefore analysed whether the state of PKR activation (phosphorylation) was dependent on the expression of ISG15. For this, the Huh7.25.CD81 cells were transfected either with siRNAs targeting ISG15 or with a plasmid expressing an HA-ISG15 construct and PKR phosphorylation was analysed as described previously [8]. The results showed that depletion of ISG15 inhibits PKR activation in the HCV-infected cells, while its overexpression stimulates it (**Figure 3D** and **Figure S5**). Therefore these data reveal that, in addition to negatively controlling RIG-I ubiquitination, ISG15 can also positively control PKR activity. The conjugation of both effects results in an efficient control of IFN induction during HCV infection.

## HCV triggers a PKR-dependent pathway early in infection to induce ISG15 and other genes

The Huh7.25.CD81 cells express ISG15 at significant basal levels. This situation was not surprising as various cellular systems can also express some of the ISGs at basal level. Expression of ISG15 was approximately 2- and 5-fold higher in the Huh7.25.CD81 cells than in the Huh7.5 or Huh7 cells (data not shown). Intriguingly however, we noticed that ISG15 expression was increased in response to HCV infection (see **Figure 2E**). To investigate this further, we simply re-used the RNAs prepared for the experiment shown in Figure 3B and performed a quantitative kinetics analysis. The results confirmed that HCV can trigger induction of ISG15 (**Figure 4A**). Unexpectedly, analysis of the RNA extracted from the cells treated with siRNAs targeting PKR, revealed that ISG15 RNA expression was strongly repressed when PKR was silenced (**Figure 4A**). This surprising result was confirmed by analysing induction of ISG56, another early ISG [26], both at the level of its endogenous RNA (**Figure 4B**) or by using an ISG56-luciferase vector (**Figure 4C**). In the latter case, a strong increase of the reporter expression in the cells treated with siRNAs targeting ISG15, was similar to the situation observed for IFNβ RNA (**Figure 2B and 2C**). This can be related to activation of the RIG-I pathway, which can function when ISG15 is absent. These data suggest that HCV may use PKR to activate gene transcription. Importantly, this phenomenon was specific to HCV as infection with Sendai virus resulted in a similar induction of ISG15 and ISG56, regardless of PKR (**Figure 4D and Figure S6**). We then examined whether overexpression of PKR could boost induction of ISG15 during HCV infection and how this would affect HCV replication and IFN induction, in relation to the pro-HCV action of ISG15. Huh7.25.CD81 cells were transfected with a plasmid expressing PKR alone or in presence of siRNAs targeting ISG15, before being infected with HCV over 48 hours. Overexpression of PKR increased the ability of HCV to induce ISG15 and concomitantly, led to an increase in HCV RNA expression. The latter increase was abolished when ISG15 was silenced, thus showing that the PKR-dependent increase in HCV expression is mediated by ISG15 (Figure **4E**). However, while the

cells silenced for ISG15 are able to induce IFN in response to HCV infection, as shown in Figure 3B, they are unable to do so when PKR is overexpressed. This suggests that PKR may also interfere with the process of IFN induction, independently of ISG15, a possibility that remains to be explored.

A role for PKR in gene induction in response to HCV infection has not been described before. Additional information was therefore obtained through a transcriptome analysis of 2165 genes in the Huh7.25.CD81 cells treated with control siRNAs or siRNAs targeting PKR and infected with HCV for 12 hrs. Out of the most significant 422 genes that were identified, 99 were unmodified or barely modified and 33 were down-regulated, while 290 genes were found to be up-regulated by HCV infection (data not shown). Among those, HCV infection triggered up-regulation of 49 genes which are directly dependent on PKR expression (**Table 1**). Forty percent of these genes (20) belong to the family of the ISGs, with ISG15 among the most induced genes (**Table 1**). In the reciprocal situation, only 17 genes depended on PKR for their down-regulation by HCV infection, with no link to a particular family of genes and limited variation both in number and intensity (**Table S1**). Thus, induction of ISGs upon HCV infection may occur through a novel signaling pathway that involves PKR.

## Induction of ISG15 by HCV is independent of RIG-I, involves MAVS/TRAF3 association with PKR and involves the DRBD region but not the catalytic activity of PKR

Infection with RNA viruses or transient transfection with dsRNA can directly and rapidly induce early ISGs, such as ISG15, through IRF3, after activation of the RIG-I/MAVS pathway and recruitment of TRAF3, an essential adapter which recruits the downstream IRF3 kinases TBK1/IKKε. We have shown that the RIG-I pathway was not operative during HCV infection in the Huh7.25.CD81 cells, precisely due to the presence of ISG15. To determine how ISG15 induction through PKR relates to or differs from the RIG-I/MAVS pathway, the Huh7.25.CD81 cells were treated with siRNAs aimed at targeting separately PKR, RIG-I, MAVS, TRAF3 and IRF3 (**Figure S7**) and infected with HCV. The results clearly showed that induction of ISG15 in response to HCV infection depends on PKR, MAVS, TRAF3 and IRF3 but not on RIG-I (**Figure 5A**). The participation of IRF3 was further confirmed by immunofluorescence studies which showed its nuclear translocation at 6 hours post-infection (**Figure S8**). ISG15, as well as ISG56, was also clearly induced in response to HCV infection in two other HCV permissive cell lines, such as Huh7 and Huh7.5 cells, and this induction was abrogated in presence of siRNAs targeting PKR (**Figure 5B and Figure S9**). Importantly, since Huh7.5 cells express a non-functional RIG-I/MAVS pathway due to a mutation in RIG-I, result with these cells supports the notion that the ability of HCV to trigger induction of ISGs through PKR is independent of RIG-I. To have more insights on this novel PKR signaling pathway, PKR was immunoprecipitated at early times points following infection of Huh7.25.CD81 cells with HCV and the immunocomplexes were analysed for the presence of MAVS, TRAF3 and RIG-I. Both MAVS and TRAF3, but not RIG-I, associate with PKR in a time dependent manner, beginning at 2 hrs post-infection (**Figure 5C**). Strikingly, these associations were abrogated by the cell-permeable peptide PRI which is analogous to the first dsRNA binding